



**Ana Isabel Costa
Calejo**

**O efeito do alumínio em células individualizadas
da hipófise anterior do rato**

**A single cell study of aluminium effect on rat
anterior pituitary**



**Ana Isabel Costa
Calejo**

**O efeito do alumínio em células individualizadas
da hipófise anterior do rato**

**A single cell study of aluminium effect on rat
anterior pituitary**

Dissertação apresentada à Universidade de Aveiro para cumprimento dos requisitos necessários à obtenção do grau de Mestre em Biologia, realizada sob a orientação científica da Doutora Maria Paula Polónia Gonçalves, Professora Associada do Departamento de Biologia da Universidade de Aveiro.

o júri

presidente

Professora Doutora Maria de Lourdes Gomes Pereira
professora associada com agregação da Universidade de Aveiro.

Professora Doutora Maria Paula Polónia Gonçalves (Orientadora)
professora associada do Universidade de Aveiro

Professor Doutor Michael Schrader
investigador principal com habilitação, da Universidade de Aveiro

agradecimentos

À Professora Doutora Maria Paula Polónia Gonçalves um agradecimento pelo apoio e orientação científica desta tese de mestrado, cuja revisão atenta e análise detalhada tornaram possível este trabalho. Desde o início do trabalho sempre se colocou à minha disposição, aconselhou, explicou e demonstrou os caminhos a seguir.

Um agradecimento especial à Professora Doutora Conceição Santos e ao Eleazar Rodrigues pelo apoio com a técnica de Citometria de Fluxo. Assim, como ao Professor Doutor Robert Zorec e ao Jernej Jorgacevski por sempre me receberem bem e pela ajuda com a electrofisiologia.

Aos meus colegas de trabalho agradeço pelo constante apoio e encorajamento. Pela ajuda prestada em todos os momentos.

Ao GRICES, Gabinete de Relações Internacionais da Ciência e do Ensino Superior, pertencente à Fundação para a Ciência e Tecnologia, pelo apoio financeiro, que tornou possível as deslocações à Eslovénia.

Aos meus eternos amigos, do Porto e Aveiro, que sempre estão presentes nos momentos bons e mais difíceis, sempre com uma palavra amiga. Especialmente à Daniela e à Ana, obrigado por desde sempre serem minhas amigas.

Um muito obrigado ao Filipe por em todos os momentos estar ao meu lado. Pela amizade que demonstrou em todas as ocasiões, sempre com uma palavra de força, encorajamento, apoio e com muita paciência. Por me ajudar e apoiar em todos os momentos e decisões.

Por último, gostaria de agradecer à minha família. Aos meus pais e irmã pelo paciência que sempre me dispensaram e foram tão decisivos na concretização deste trabalho. Pelo apoio em todos os momentos um muito obrigado.

palavras-chave

Toxicidade do alumínio, viabilidade celular, exocitose regulada, propriedades do poro de fusão, cultura de células da hipófise anterior do rato enriquecidas em lactotrofos.

resumo

O alumínio foi pela primeira vez reconhecido como um agente neurotóxico para o Homem em 1886. Uma vasta gama de efeitos tóxicos do alumínio a nível celular foi já demonstrada, no entanto permanece desconhecido o modo como o alumínio afecta as células da hipófise anterior. A exposição ocupacional a alumínio pode causar redução dos níveis séricos de prolactina, uma hormona peptídica sintetizada e secretada principalmente pelas células lactotropas hipofisárias. O principal objectivo deste trabalho foi estudar o efeito do alumínio na viabilidade celular e na actividade exocitótica em culturas de células da hipófise anterior do rato enriquecidas em lactotrofos. A quantificação das células vivas e mortas foi realizada por citometria de fluxo após dupla marcação com sondas fluorescentes. Observámos uma diminuição significativa na viabilidade celular após 30 min de exposição a 300 μM de AlCl_3 . Uma concentração dez vezes menor causou perda significativa de células apenas após 4 dias de exposição. Para exposições prolongadas a concentrações inferiores a 30 μM , a viabilidade celular manteve-se elevada. A morte celular induzida por alumínio parece ser precedida pela sua acumulação nas células, visto que a análise por espectrometria de absorção atómica relevou um aumento significativo de Al^{3+} nos lactotrofos após 1h de exposição à menor concentração com efeito na viabilidade (30 μM AlCl_3). Os efeitos subletais do AlCl_3 na exocitose regulada foram avaliados com recurso a métodos de electrofisiologia celular. O registo com elevada resolução das alterações de capacitância e condutância da membrana celular permitiu diferenciar eventos de fusão singelos entre vesículas de secreção e a membrana plasmática em condições espontâneas e durante estimulação. Após 24 h de exposição a 30 μM AlCl_3 , a resposta exocitótica à estimulação foi reprimida e verificaram-se diferenças nas propriedades dos poros de fusão. Actualmente considera-se que durante a exocitose regulada e reversível ocorre secreção do conteúdo vesicular através do poro de fusão, o qual é formado pelas membranas vesicular e plasmática. Após a exposição ao alumínio os poros de fusão, observados durante o processo de fusão reversível ("kiss-and-run") revelaram-se mais estreitos, visto que as suas condutâncias eram inferiores às registadas durante os eventos espontâneos ocorridos em condições fisiológicas normais. Estes resultados levam os autores a sugerir que (1) concentrações subletais de alumínio tornam a exocitose regulada improdutivo, de tal modo que grandes moléculas, como a prolactina, não conseguem ser secretadas e que (2) a perda de células lactotropas hipofisárias poderá ocorrer devido a exposição a este agente neurotóxico.

keywords

Aluminium toxicity, cell viability, regulated exocytosis, fusion pore properties, rat anterior pituitary lactotrophs-enriched culture.

abstract

Aluminium was first recognized as a human neurotoxic agent in 1886. Besides a wide range of toxic effects of aluminium have been demonstrated at cellular level, how it affects anterior pituitary cells remains unknown. It was shown that workers exposed to aluminium presented lower levels of serum prolactin, a peptide hormone mainly synthesised and secreted by anterior pituitary lactotrophs. The aim of this work was to study the aluminium effect on cell viability and regulated exocytotic activity in rat pituitary lactotrophs-enriched cultures. Dual-labeling flow cytometric assays were performed to quantify live and dead cells simultaneously. We observed a significant decrease of cell viability following 30 min-exposure of cell cultures to 300 μM AlCl_3 . At a ten-fold lower concentration, overt cell lost was only achieved by extending exposure time to 4 days. For continuous exposure to AlCl_3 concentrations lower than 30 μM , even for prolonged periods of up to 4 days, enriched cultures of pituitary lactotrophs maintained high levels of viability. Aluminium-induced cell lost seems to be headed by its cellular accumulation, given that atomic absorption spectrometry analyses revealed a significant increase of Al^{3+} retention by lactotrophs after 1h-exposure to the lowest concentration with effect in viability (30 μM AlCl_3). The sublethal effect of AlCl_3 on the regulated exocytosis by rat pituitary lactotrophs was assessed by patch-clamp cell-attached technique. We performed high-resolution membrane capacitance and conductance measurements to resolve unitary fusion events of large dense-core vesicle with the plasma membrane under spontaneous and stimulated conditions. After 24-h exposure to 30 μM AlCl_3 , exocytotic response to stimulation was repressed and differences in elementary fusion pore properties were detected. The transient fusion pore of regulated exocytosis is believed to be an aqueous channel that connects and spans the vesicle and the plasma membrane, through which the content of secretory vesicle may be released. Following exposure to aluminium fusion pores, seen during reversible fusion process (kiss-and-run), appeared narrower, since they had lower conductance than that of resting values under normal physiological conditions. These results lead the authors to suggest that (1) sublethal aluminium concentrations shift the mode of regulated exocytosis to unproductive such that large cargo molecules like prolactin cannot be secreted and (2) lactotroph lost at the anterior pituitary might occur due to exposure to this neurotoxic agent.

Index

	Page
Abbreviations	1
I. Cell death induced by aluminium in rat pituitary lactotroph-enriched culture	3
1. Introduction	5
2. Materials and methods	9
2.1 .Cell culture and aluminium exposure	9
2.2. Cell viability assays	9
2.3. Aluminium quantification	10
2.4. Data analysis	11
3. Results and discussion	13
3.1. Definition of cell subpopulations from rat anterior pituitary lactotroph-enriched cultures	13
3.2. Susceptibility of rat anterior pituitary lactotroph-enriched cultures to AlCl ₃	17
4. References	23
II. Aluminium effect in elementary exocytotic events of rat pituitary lactotroph-enriched culture	29
1. Introduction	31
2. Materials and methods	35
2.1 .Cell culture and aluminium exposure	35
2.2. Electrophysiology	35
2.3. Data analysis	36

3. Results and discussion	37
3.1. Capacitance measurements of spontaneous fusion events after exposure to AlCl_3	37
3.2. Frequency of stimulated fusion events after exposure to AlCl_3	39
3.3. AlCl_3 effect on the profile of “kiss-and-run” fusion events	41
3.4. AlCl_3 effect on fusion pore properties	42
4. References	49
III. Conclusion	57

Abbreviations

C_m	Membrane capacitance
C_v	Vesicle capacitance
EthD-1	Ethidium homodimer 1
G_p	Pore conductance
I_m	Imaginary trace
LDCV	Large-dense-core vesicles
LDH	lactate dehydrogenase
PIP ₂	phosphatidylinositol 4,5-bisphosphate
R_e	Real trace
SV	Small vesicles

I. Cell death induced by aluminium in rat pituitary lactotroph-enriched cultures

1. Introduction

More than 25 years has passed since the first report about the association of aluminium with human neurodegenerative diseases (Perl, 1980). Some lines of evidence suggest that accumulation of aluminium is a common feature of the intraneuronal protein aggregations seen in association with age-related neurodegenerative disorders (McDermott *et al.*, 1979; Roberts *et al.*, 1998; Savory *et al.*, 2001; Perl and Moalem, 2006). Many malfunctions described in human neurodegenerative diseases seem to be mimicked by direct injection of aluminium compounds into rabbit central nervous system (Savory *et al.*, 2001).

The continuing controversy over exposure to aluminium and neurodegeneration has rocked research on aluminium-induced cell death, given that neuronal loss occurs during neurodegeneration. Once again numerous studies have revealed no conclusive evidence for aluminium-induced highly specific neuron loss or neuronal cell death in particular brain regions. For instance, exposure of cell cultures of rat hippocampus and human cerebral cortex to cultures to 200 μM Al^{3+} for up to 6 days did not induce neuronal degeneration (Mattson *et al.*, 1993). On the contrary, in the range of micromolar concentrations, AlCl_3 accelerates apoptosis in cultured rat cortical neurons, and its effect seems to involve the stress-activated protein kinase / c-jun N-terminal kinase signal transduction pathway (Fu *et al.*, 2003). Savory and co-workers hypothesised that aluminium induces neuronal apoptosis by its effects on functioning of both the endoplasmic reticulum and mitochondria, based on extensive study of neuronal injury resulting from the administration of aluminium maltolate, via the intracisternal route, to New Zealand white rabbits (review in Savory *et al.*, 2003). Aluminium-induced apoptosis in other experimental models has been also demonstrated by other investigators. U 373MG glioblastoma cells showed significant activation of the apoptotic enzyme caspase 3 with a peak after 24h incubation time at 1 μM AlCl_3 (Toimela and Tahti, 2004). In the same study, the authors showed that overt sign of apoptosis appeared more slowly and with higher concentrations in the D407 retinal pigment epithelial cell line, whereas aluminium chloride failed to induce apoptosis in SH-SY5Y neuroblastoma cell cultures. Several lines of evidence support neuronal cell loss dependency upon the presence of astrocytes rather than a direct effect on neuronal cells. During prolonged exposure to millimolar aluminium extensive degeneration of cerebellar neurons was only observed when neurons were co-cultured with astrocytes (Suárez-Fernández *et al.*, 1999). Tight metabolic linkage between neurons and astrocytes has been identified as crucial during

glial-mediated neurotoxicity of aluminium (Platt *et al.*, 2001; Aremu and Meshitsuka, 2005; Meshitsuka and Aremu, 2008). Recently, a protective role for astrocytes during aluminium-induced neuronal cell loss has been proposed, given that the intensity of apoptosis was much less in neuron/astrocyte co-cultures than in primary neurons cultured alone (Zhang *et al.*, 2008). In matter of fact, depending on specific ligand concentration and period of exposure, aluminium can lead or not to cell death by apoptosis or by necrosis (Lévesque *et al.*, 2000; Deloncle *et al.*, 2001; Guo and Liang, 2001; Johnson *et al.*, 2005; Meshitsuka and Aremu, 2008).

It is well-known that aluminium can cross and alter the blood–brain barrier (reviewed in Yokel, 2002) and also that differentiated distribution and accumulation of aluminium in the distinct brain areas depends on the route of exposure (Zatta *et al.*, 1993; Priest, 2004; Sánchez-Iglesias *et al.*, 2007). The toxicity of aluminium has been widely shown in multiple studies on extraneural tissues, attesting its harmful effects in multiple organs (reviewed in Nayak, 2002). Even though very little information has been published about aluminium effect on pituitary gland. An “in vivo” study revealed a significant enhancement of aluminium concentration in the pituitary gland when compared to other organs (rib > tibia > liver > kidney > spleen > pituitary gland > brain) in wethers treated with aluminium citrate (Allen *et al.*, 1991). Aluminium accumulation in the cytoplasm of anterior pituitary cells has also been documented by Walton (2004). Moreover, subcutaneous ²⁶Al injection of lactating rats causes incorporation of ²⁶Al in the several organs of sucklings, probably via maternal milk (Yumoto *et al.*, 2001).

Prolactin has more effects than all other pituitary hormones combined and is of great importance in reproduction (review in Bole-Feysot *et al.*, 1998). It is well known that aluminium has an enormous variety of adverse effects in reproduction. Among other effects aluminium interferes with pre- and postnatal development and behaviour of offsprings, progress of pregnancy, male sexual behaviour and production of sexual hormones (Agarwal *et al.*, 1995; Domingo, 1995; Domingo *et al.*, 2000; Nayak, 2002). The control of these physiological processes is participated by prolactin (review in Bole-Feysot *et al.*, 1998). Alessio and co-workers found reduced prolactin levels in subjects with occupational exposure to aluminium (Alessio *et al.*, 1989). Circulating prolactin originates mostly from pituitary lactotrophs, which represent the most abundant cell population of the rat anterior pituitary (review in Burrows *et al.*, 1999).

The present study aimed to investigate the effect of aluminium on cell viability in rat pituitary lactotrophs-enriched cultures. For this purpose, dual-labelling flow cytometric assays were performed to evidence the time and concentration dependences of cell death

induced by AlCl_3 . Inspection of stained cells by inverted microscopy and lactate dehydrogenase leakage assays were carried through for confirmation of the results. Additionally, atomic absorption spectrometry analyses was undertaken to demonstrate cellular retention of Al^{3+} following exposure of rat pituitary lactotroph-enriched cultures to AlCl_3 .

2. Materials and methods

2.1. Cell culture and aluminium exposure

Male Wistar rats were handled in accordance with guidelines for the accommodation and care of animals used for experimental and other scientific purposes (Official Journal of the European Union L197 of 30.7.2007). Primary cultures were obtained from the anterior pituitaries as described previously (Ben-Tabou *et al.*, 1994). The rat pituitary lactotroph-enriched cultures, maintained either in suspension or plated on poly-L-lysine coated glass coverslips, were stored at 37°C, 92% humidity and 5% CO₂ in high-glucose DMEM buffered with HEPES-Tricine and supplemented with 1.5 µM BSA, 2 mM L-glutamine and 1% newborn calf serum. The incubation medium was changed every second day and experiments were carried out at room temperature 1 to 4 days after the isolation.

Primary rat pituitary lactotroph-enriched cultures were exposed to different concentrations of AlCl₃ (0 – 30 mM) either in the above mentioned incubation medium or in buffered (10 mM HEPES/NaOH at pH 7.2) saline solutions containing 10 mM D-glucose, 8 mM CaCl₂ and 1 mM MgCl₂ surplussed with 130 mM NaCl and 5 mM KCl (extracellular medium) or with 100 mM KCl and 35 mM NaCl (stimulating medium) as mentioned in the legends of the respective figures. The cell cultures were maintained in the incubator (37°C, 92% humidity and 5% CO₂) all over the period of aluminium exposure, which lasted for 30 min up to 4 days.

2.2. Cell viability assays

Cell viability was determined using the LIVE/DEAD viability/cytotoxicity kit for mammalian cells from Molecular Probes according to the flow cytometry protocol provided by the manufacturer. After incubation of the cell suspensions with ethidium homodimer-1 (EH-1) and calcein-AM for 15 min, the cells ($\approx 8 \times 10^5$ cells/ml) were analyzed in a Coulter EPICS XL (Coulter Electronics, Hialeah, FL, USA). All measurements were made using the 488-nm line from a 15 mW air-cooled argon-ion laser. The intensity of forward and side-scattered light as well as green and red fluorescence was quantified. The green and red fluorescence emitted by calcein-AM and EthD-1 were measured using a 525 band-pass filter and 620 band-pass filter, respectively. Correlated measurements on at least 2000 events per sample were acquired and stored by SYSTEM II version 3_0 (Coulter

Electronics) software. The list mode data were processed as parameter frequency distribution histograms and diagrams formed by bivariate combinations of the above parameters by using the WinMDI 2.9 software. The same two-colour fluorescence cell viability assay was also used with cell cultures plated on poly-L-lysine coated glass coverslips. Labelled cells were then viewed under the fluorescence inverted microscope. Images were acquired by using a Zeiss (Jena, Germany) AXIO Observer microscope equipped with a System TILL Photonics using the software TILLvisION (Munich Germany). We used 494 nm and 528 nm laser excitation and band-pass filters of 515 and long-pass 590 nm. Images were exported and further visually analyzed with Adobe Photoshop CS2 software.

The kit “Enzyline LDH/HBDH Optimisé Unitaire” (BioMérieux) was employed to assay lactate dehydrogenase leakage (LDH) from cells. Briefly, cell suspensions were incubated in extracellular solution and then pelleted by centrifugation at 230 xg for 5 min. Supernatants were assayed for LDH activity and the pellets were incubated in 10 mM HEPES- Tris (pH 7.4) and 1% Triton X-100 to promote total LDH release. After centrifugation (230 xg for 5 min) the supernatants were assayed for LDH activity. LDH activity was measured spectrophotometrically at 340 nm by following the oxidation of NADH (decrease in absorbance) in the presence of pyruvate using a spectrophotometer UV/VIS “Perkin-Elmer, model Lambda 14 P”. LDH leakage was expressed as a percentage of the total LDH activity in the cell suspensions.

2.3. Aluminium quantification

Aluminium measurements in cell extracts were performed by graphite furnace atomic absorption spectrometry (GFAAS). The glass and polyethylene material was washed with nitric acid 10% (v/v) and ultra-pure water, in order to reduce the contamination with aluminium. Briefly, cell suspensions ($\approx 6 \times 10^5$ cells/ml) were incubated with chilled extraction solution (4% TCA prepared in 0.1 N nitric acid) during 30 min. The samples were centrifuged at 6,000 xg for 10 min and the concentration of Al^{3+} concentration in the supernatants was measured at 309.3 nm using a “Perkin Elmer 4100” atomic absorption spectrometer with graphite furnace and AS-70 autosampler. The aluminium concentration in anterior pituitary cells was expressed as ng Al^{3+} /ml of cell suspension.

2.4. Data analysis

All results are presented as mean \pm standard error of the mean (SEM) of the number of experiments indicated in the legends of the figures. Statistical significance was evaluated by Student's t-test and p values are presented in the figures.

3. Results and discussion

3.1. Definition of cell subpopulations from rat anterior pituitary lactotroph-enriched cultures

Flow cytometry was chosen since it is a very fast and sensitive technique for examining cell suspensions that can provide functional and structural information of each individual cell. After isolation, the primary rat anterior pituitary cultures enriched in lactotrophs were maintained in suspension in DMEM growth medium at 37°C and 5% CO₂ and examined periodically by flow cytometry technique. At multiple time points, cell aliquots ($\approx 8 \times 10^5$ cells/ml) were analysed for forward and side light scattering and logarithmic amplification was used to measure fluorescence in cells after staining with the vital dyes, calcein-AM and ethidium homodimer 1 (EthD-1). Light scattering reflects general cell properties such as size and shape, since it has been previously proposed that forward angle light scattering (FSC) is proportional to cell surface area or size and side angle light scattering (SSC) is proportional to cell granularity or internal complexity (Salzman *et al.*, 1975). On the other hand, dual-labelling flow cytometric assays allows to determine simultaneously live and dead cells within an entire population. EthD-1 is a cell-impermeant, nucleic acid intercalating dye, which strongly binds to double-stranded DNA (dsDNA), single-stranded DNA (ssDNA), RNA and oligonucleotides. In contrast, the cell-permeant probe calcein AM is converted by the intracellular esterase activity to the polyanionic dye calcein that is retained within live cells. Therefore, intracellular esterase activity and plasma membrane integrity were measured, which are two recognized parameters of cell viability.

As it can be seen in Fig. 1A, the primary rat anterior pituitary cultures enriched in lactotrophs exhibited some degree of heterogeneity, which was mainly due to cell damage caused by manipulation and the occurrence of multicell aggregates, since it is difficult to prepare suspensions of truly single cells from anterior pituitary without damaging cells. Thereby, analyzed cells were compared to size-calibrated polystyrene latex spheres (Agar Scientific Limited; Essex, England) and gated according to their FSC and SSC plot. After microscopic examination of double-labelling cell cultures, cell debris and multicell aggregates were excluded by appropriated fluorescence and light-scattering threshold setting (Fig. 1F).

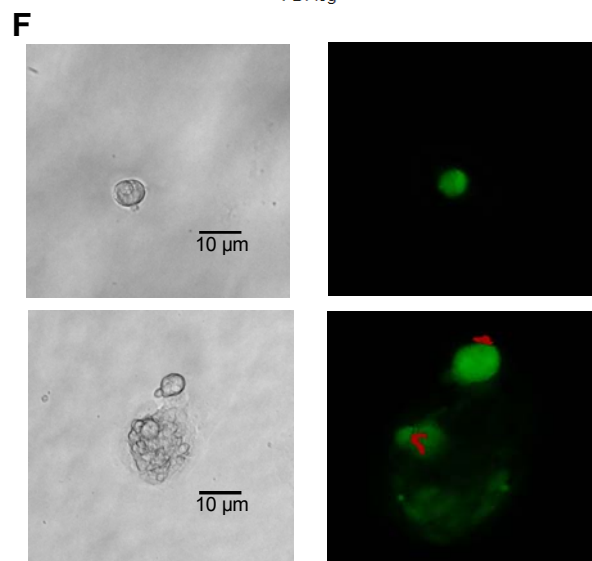
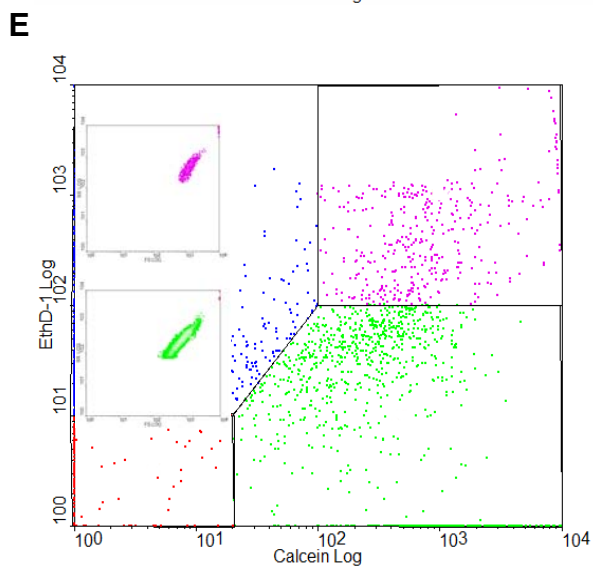
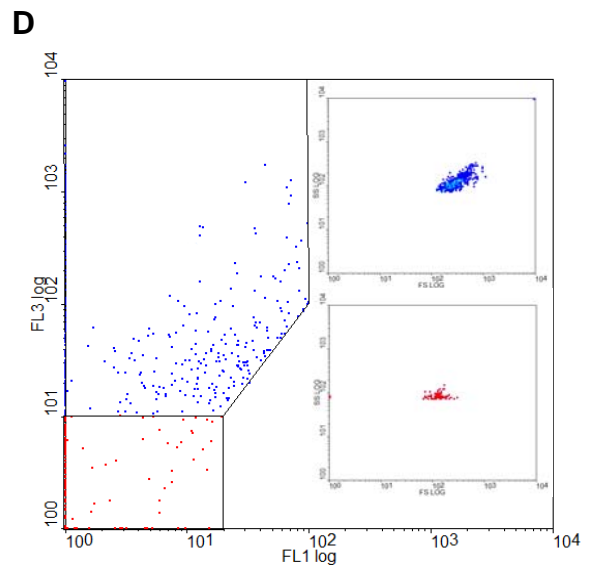
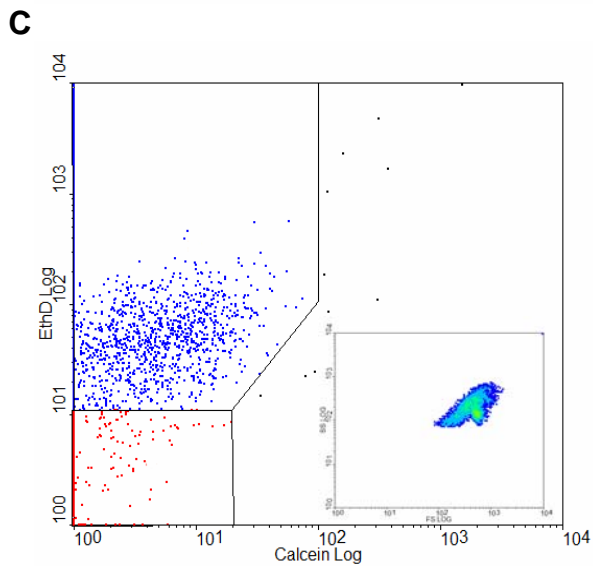
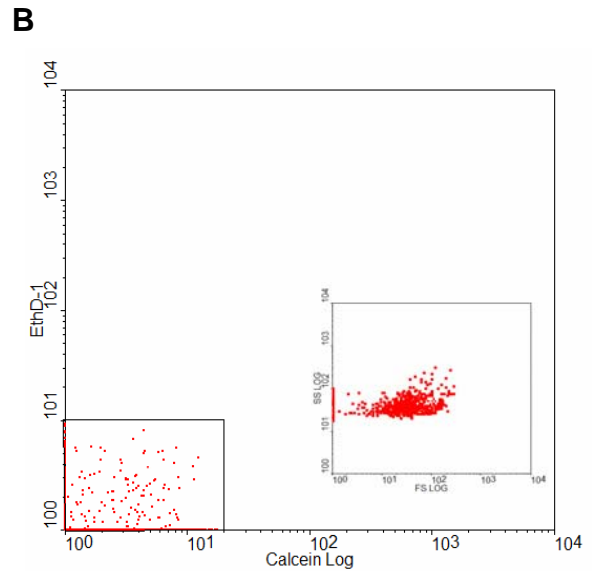
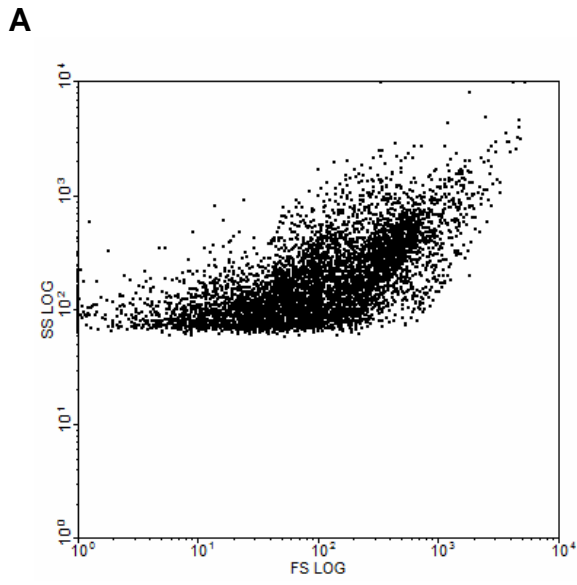


Figure 1. Application of flow cytometric method to analyze cell subpopulations in rat anterior pituitary lactotrophs-enriched cultures according to survival level.

Cell suspensions were analyzed by flow cytometry as described in “Materials and methods”. Cell population was gated by light scattering properties in order to establish a window of analysis and exclude cellular debris (**A**). Cell subpopulations were selected considering their fluorescence properties (**B-E**). Unlabeled cells and remained cellular debris (red dots), death cells (blue dots), live cells (green dots) and multicell aggregates containing both death and live cells (purple dots) are shown in illustrative bivariate displays representing cell suspensions. **B**, no fluorescence label; **C**, two fluorescence labels (calcein AM and EthD-1) after permeabilization with 1% Triton X-100; **D**, one fluorescence label (EthD-1); and **E**, two fluorescence labels (calcein AM and EthD-1). SSC/FCS density plots of each subpopulation are displayed as insets. Panel **F** shows microscopy images of a single cell stained with calcein and double-labelling multicell aggregates.

Four quadrants of the cytograms were set using negative controls. The bottom left quadrant showed a small percentage of unmarked cells and cell debris, since these low fluorescent events mainly clustered as $FCS^{low}SSC^{low}$ (Fig. 1B). The upper left quadrant showed cells which had lost their plasma membrane integrity and were stained only by EthD-1 (Fig. 1D). In matter of fact, the FCS/SSC and fluorescence profiles of cells permeabilized with 1% Triton X-100 and incubated with both, calcein-AM and EthD-1, resolved into two areas: an $EthD-1^{low}FCS^{low}SSC^{low}$ and an $EthD-1^{mid-high}FCS^{mid-high}SSC^{low}$ area (Fig. 1C). The right quadrants showed (Fig. 1E) truly calcein stained cells, it means viable cells with preserved plasma membrane integrity. However, these cells could be depicted into two subpopulations according to the level of EthD-1 staining. Thereby, the bottom right quadrant shows $Calcein^{mid-high}EthD-1^{low-mid}$ profile, whereas the upper right quadrant shows $Calcein^{high}EthD-1^{high}$ profile. Because dead and live cells may coexist within multicell aggregates and failing cells may contain structures with increased light scattering properties clearly before completely lost of their plasma membrane integrity, the FCS/SSC profiles of these two subpopulations were also analysed and microscopic examination was performed. As it can be observed, the $Calcein^{high}EthD-1^{high}$ profile (upper right quadrant) represents a subpopulation with $FCS^{high}SSC^{high}$ profile, whereas the $Calcein^{mid-high}EthD-1^{low-mid}$ subpopulation (bottom right quadrant) exhibited a $FCS^{mid}SSC^{mid}$ profile. Additionally, aggregates composed by green (Calcein staining) and red (EthD-1 staining) cells as well as some few cells exhibiting apparently both staining have been observed. Accordingly, only the bottom right quadrant has been considered as representing viable cells dispersed in the suspension.

The fraction of live cells in each cell culture was calculated by dividing the number of events in the bottom right quadrant by the total number of events in the right quadrants

plus those in the upper left one (Fig. 2A). The cell viability, expressed as the percentage of live cells, has been estimated to be $67 \pm 3 \%$ when cell suspensions were maintained under optimal cell culture conditions. Most likely this method of calculating the cell viability raised underestimated values, given that double staining events (upper right quadrant) represented as much as $15 \pm 2 \%$ (2060 ± 575 ; $n = 11$ cell cultures) of the total account.

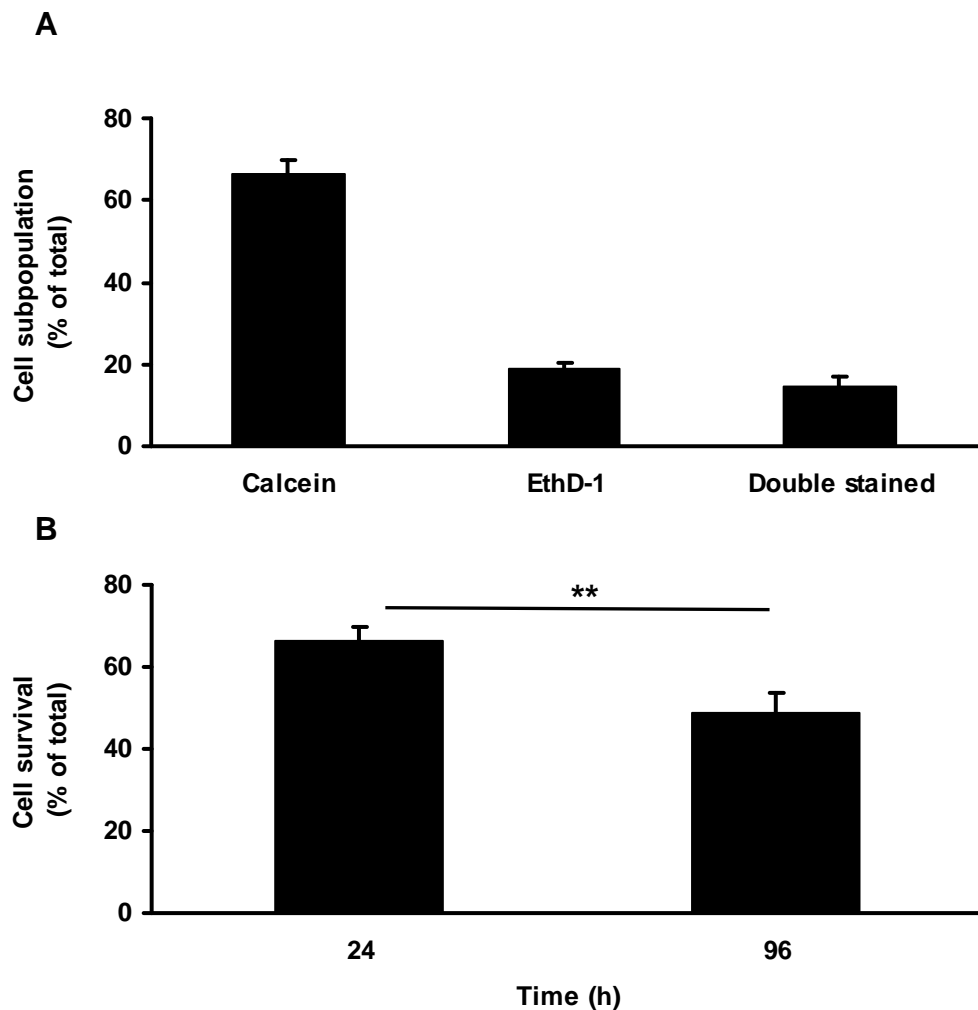


Figure 2. Cell survival under the standard protocol for maintenance of lactotroph-enriched cultures

Relative calcein and EthD-1 staining of anterior pituitary cells incubated for 24h (A) at 37°C and 5% CO₂. Cells were analyzed by flow cytometry as described in “materials and methods”. Vertical bars denote SEM. of at 11 independent experiments. (B) Cell survival after 24h and 96h at 37°C and 5% CO₂. Vertical bars denote SEM of 2 independent experiments. ** $p < 0.02$, when comparing incubation of 24 and 96h.

This hypothesis was further corroborated by using LDH leakage as a marker for cell viability. The LDH leakage assay is both sensitive as an indicator of membrane

damage and insensitive to the presence of multicell aggregates. Cell viability was estimated to be $83 \pm 1 \%$ when measured by LDH leakage assay. The relative viable cell count on day 4 after incubation of the cell suspensions started to decline, thereby all exposure protocols were conducted within such time period (Fig. 2B).

3.2. Susceptibility of rat anterior pituitary lactotroph-enriched cultures to AlCl_3

Exposure to AlCl_3 of rat anterior pituitary lactotroph-enriched cultures significantly decreased cell viability in a concentration dependent manner as assessed using dual-labeling flow cytometry (Fig. 3). Cells were exposed to increasing AlCl_3 concentrations ($0.3 \mu\text{M}$ – 30 mM) on day 1 of culture and after incubation during 24 h cell viability was evaluated as previously described.

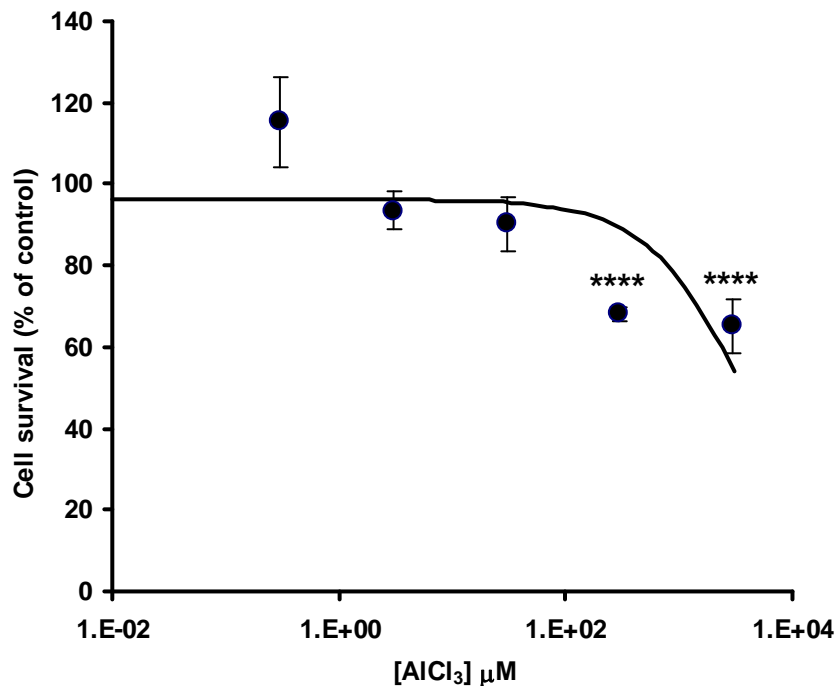


Figure 3. Concentration dependence of the aluminium-induced cell death.

Cell suspensions were incubated for 24h with increasing concentrations of aluminium (0 - 3 mM) at 37°C and 5% CO_2 . Cells were analyzed by flow cytometry as described in “Materials and methods”. Vertical bars denote SEM of at least 2 independent experiments. **** $p < 0.001$, compared to control of the same batch (absence of aluminium).

For clarity, cell survival upon exposure to aluminium was expressed as a percentage of the control (cell suspensions from the same batch of primary cultures that

were maintained under the same culture conditions but in the absence of added AlCl_3) levels which were set at 100%.

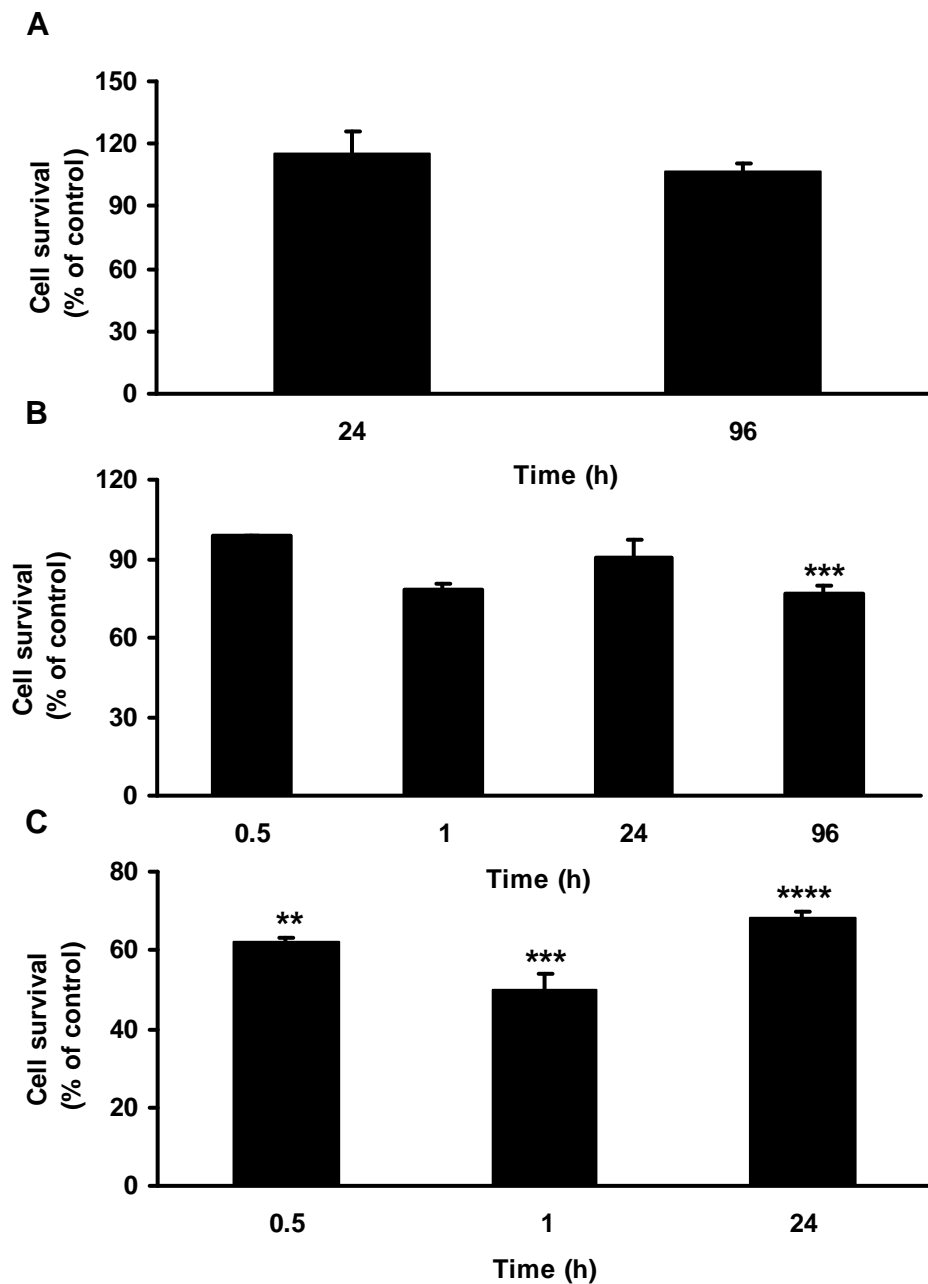


Figure 4. Stability of the aluminium effect over time.

Cell suspensions were incubated for different times (0.5, 1, 24 and 96 h) in presence of 0.3 μM (A), 30 μM (B) and 300 μM (C) AlCl_3 at 37°C and 5% CO_2 . Cells were analyzed by flow cytometry as described in "Materials and methods". Vertical bars denote SEM of at least 2 independent experiments. ** $p < 0.02$, *** $p < 0.01$ and **** $p < 0.001$, compared to control of the same batch (absence of aluminium).

Aluminium-induced cell death could not be determined for AlCl_3 concentrations higher than 3 mM due to metal precipitation. For concentrations below this threshold the excitation and emission spectra of either calcein or EthD-1 remained unchanged (data not shown). As it can be observed in Fig. 3, AlCl_3 concentrations of 0.3, 3 and 30 μM did not alter cell survival. One, 0.3 and 3 mM were significantly different from the unexposed group ($p < 0.001$). To determine if there was an overall effect of time on aluminium-induced cell death, cell viability was examined in suspensions following aluminium injury for varying lengths of incubation (Fig. 4). Exposure to 0.3 μM AlCl_3 did not induce cell death at any time sampled (Fig. 4A). In the presence of 30 μM AlCl_3 , a progressive increase of cell death reaching statistical significance at 4 days compared to the respective timepoint control was observed (Fig. 4B). It is important to note that cell death induced by 30 μM AlCl_3 was preceded by accumulation of Al^{3+} , as ascertained by graphite furnace atomic absorption spectrometric analysis. Following exposure as brief as 1 h, an enrichment on Al^{3+} of 57 ng/ml of cell suspension was detected yet no statistically significant ($p = 0.35$) change was surveyed in the extension of aluminium-induced cell death (~78 % cell survival). In contrast, the fold tolerance to a ten-fold higher concentration of AlCl_3 (300 μM) at 24 h of exposure could be already detected as early as after 30 min exposure (Fig. 4C). Remarkably, the extent of aluminium-induced cell death remained constant (~60 % cell survival) as compared to controls at 0.5, 1 and 24 h and being statistically significant from the 30 min timepoint.

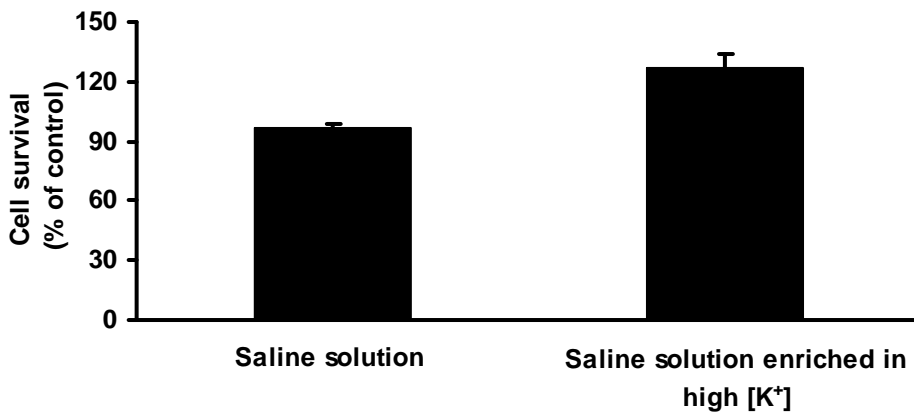


Figure 5. Impact of lactotroph stimulation on aluminium-induced cell death.

Cell suspensions were incubated with or without 300 μM AlCl_3 in saline solution enriched or not in high $[\text{K}^+]$ for 5 min at 37°C and 5% CO_2 . Media were replaced by DMEM containing or not AlCl_3 (300 μM) and after 1 h the cells were analyzed by flow cytometry as described in “Materials and methods”. Vertical bars denote SEM of at least 2 independent experiments.

It has been repetitively shown that cultured lactotrophs exhibit both spontaneous and stimulated secretion of prolactin (Stojilkovic, 2006; Jorgacevski *et al.*, 2008). The experiment depicted in Fig. 5 was performed to investigate the effect of aluminium on cell survival during the conditions usually used to promote Ca^{2+} regulated prolactin secretion in rat anterior pituitary lactotroph-enriched cultures (Stojilkovic, 2006). On day 1 of culture cells were collected by centrifugation and incubated in saline solution enriched or not on high K^+ concentration for 5 min in the absence or in the presence of $300 \mu\text{M AlCl}_3$. After media replacement by DMEM growth medium, the cell cultures were left to recover for 1 h at the incubator (37°C and $5\% \text{CO}_2$) in the absence or in the presence of $300 \mu\text{M AlCl}_3$. Dual-labeling flow cytometry analysis revealed no significant difference in cell survival between the absence or the presence of AlCl_3 . Thereby, it appears that the extent of aluminium-induced cell injury (Figs. 3 and 4) was less prominent than that caused by handling cell cultures during the performance of protocols to promote prolactin secretion under spontaneous and stimulating conditions.

Severe deleterious effects of aluminium have been most often explained by selective accumulation of this metal in particular organs and cell types (Zatta *et al.*, 1993). At cellular level, deathly effects of aluminium have been documented in neurons (Fu *et al.*, 2003; Savory *et al.*, 2003), astrocytes (Suarez-Fernandez *et al.*, 1999; Guo *et al.*, 2001) and kidney proximal tubular cells (Sargazi *et al.*, 2001). In this study we confirmed that mammalian pituitary cells can accumulate Al^{3+} as previously demonstrated using other experimental models (Allen *et al.*, 1991; Walton, 2004). Additionally, aluminium induced death of lactotrophs was shown for the first time.

Both major types of cell death, apoptosis and necrosis, appear to occur in consequence of exposure to aluminium (Lévesque *et al.*, 2000; Deloncle *et al.*, 2001; Guo and Liang, 2001; Johnson *et al.*, 2005; Meshitsuka and Aremu, 2008). In spite of much research on aluminium toxicity in mammalian cells, the exact mechanism of aluminium stress signalling to induce either apoptosis or necrosis remains unclear. It is known that other metals like chromium VI and cadmium can induce apoptosis in anterior pituitary cells via caspase 3 activation due to oxidative stress (Quinteros *et al.*, 2007; Poliandri *et al.*, 2006; Poliandri *et al.*, 2003; Quinteros *et al.*, 2008). Cadmium modifies the lipid content of pituitary gland and directly or indirectly the levels of prolactin and growth hormone in serum (Calderoni *et al.*, 2005). The aluminium-induced potentiation of transition metal prooxidant action in cell systems is well established (Boegman and Bates, 1984; Nayak and Chatterjee, 2002; Yokel, 2006). Lactotrophs in culture showed substantial decrease of

survival even after a short (30 min) exposure to 300 μM AlCl_3 , whereas more than 24 h were required to induce cell death in the presence of 30 μM AlCl_3 . Although these observations do not elucidate the type of cell death that occurs upon exposure to aluminium under our experimental conditions, they seem to suggest that the aluminium-induced cell death exhibits both apoptotic and necrotic features. In addition to new experimental approaches, further analysis of the obtained already results will reveal essential data to clarify this question.

In conclusion, aluminium induced cell death in rat anterior pituitary lactotroph-enriched cultures in a concentration and time dependent manner, suggesting that exposure to this neurotoxic agent might cause lactotroph lost at the anterior pituitary.

4. References

- Agarwal, S.K.; Ayyash, L., Gourley, C.S., Levy, J., Faber, K., Hughes C.L. 1999. Evaluation of the developmental neuroendocrine and reproductive toxicology of aluminium. *Food Chem Toxicol.* 34,49-53.
- Alessio, L., Apostoli, P., Ferioli, A., Di Sipio, I., Mussi, I., Rigosa, C. 1989. Behaviour of biological indicators of internal dose and some neuro-endocrine tests in aluminium workers. *Med Lav* 80, 290–300.
- Allen, V. G., Fontenot, J. P., Rahnema, S. H. 1991. Influence of aluminum-citrate and citric acid on tissue mineral composition in wether sheep. *J Anim Sci.* 69, 792-800.
- Aremu, D.A., Meshitsuka, S. 2005. Accumulation of aluminum by primary cultured astrocytes from aluminum amino acid complex and its apoptotic effect. *Brain Res.* 1031, 284-296.
- Ben-Tabou, S., Keller, E., Nussinovitch, I. 1994. Mechanosensitivity of voltage-gated calcium currents in rat anterior pituitary cells. *J Physiol.* 476, 29-39.
- Boegman, R.J., Bates, L.A. 1984. Neurotoxicity of aluminum. *Can J Physiol Pharmacol.* 62, 1010-1014.
- Bole-Feysot, C., Goffin, V., Edery, M., Binart, N., Kelly, P. A. 1998. Prolactin (PRL) and its receptors: actions, signal transduction pathways and phenotypes observed in PRL receptor knockout mice. *Endocrine Reviews* 19, 225-268. *Brain Res.* 1031, 284-96.
- Burrows, H.L., Douglas, K.R., Seasholtz, A.F., Camper, S.A. 1999. Genealogy of the Anterior Pituitary Gland: Tracing a Family Tree. *Trends Endocrinol Metab.* 10, 343-352.
- Calderoni, A.M., Oliveros, L., Jahn, G., Anton, R., Luco, J., Giménez, M.S. 2005. Alterations in the lipid content of pituitary gland and serum prolactin and growth hormone in cadmium treated rats. *Biometals.* 18, 213-220.

Deloncle, R., Huguet, F., Fernandez, B., Quellard, N., Babin, P., Guillard, O. 2001. Ultrastructural study of rat hippocampus after chronic administration of aluminum L-glutamate: an acceleration of the aging process. *Exp Gerontol.* 36, 231-44.

Domingo, J.L. 1995. Reproductive and developmental toxicity of aluminum: a review. *Neurotoxicol Teratol.* 17, 515-521.

Domingo, J.L., Gómez, M., Colomina, M.T. 2000. Risks of aluminium exposure during pregnancy. *Contribution to Science.* 1, 479-487.

Fu, H., Hu, Q., Lin Z., Ren T., Song H., Cai, C., Dong S. 2003. Aluminum-induced apoptosis in cultured cortical neurons and its effect on SAPK/JNK signal transduction pathway. *Brain Research.* 980, 11–23.

Guo G.W., Liang, Y.X. 2001. Aluminum-induced apoptosis in cultured astrocytes and its effect on calcium homeostasis. *Brain Research.* 888, 221–226.

Johnson, V. J., Kim, S. H., Sharma, R.P. 2005. Aluminum-maltolate induces apoptosis and necrosis in neuro-2a cells: Potential role for p53 signaling. *Toxicol. Sci.* 83, 329–339.

Jorgacevski, J., Stenovec, M., Kreft, M., Bajic, A., Rituper, B., Vardjan, N., Stojilkovic, S., Zorec, R. 2008 Hypotonicity and Peptide Discharge from a Single Vesicle. *Am J Physiol Cell Physiol.* [Epub ahead of print]

Lévesque, L., Mizzen, C.A., McLachlan, D.R., Fraser, P.E. 2000. Ligand specific effects on aluminum incorporation and toxicity in neurons and astrocytes. *Brain Res.* 877, 191-202.

Mattson, M.P., Lovell, M.A., Ehmann, W.D., Markesbery, W.R. 1993. Comparison of the effects of elevated intracellular aluminum and calcium levels on neuronal survival and tau immunoreactivity. *Brain Res.* 602, 21-31.

McDermott, J.R., Smith, A.I., Iqbal, K., Wisnieswsk, H.M., 1979. Brain aluminium imaging and Alzheimer disease. *Neurology* 29, 809-814.

Meshitsuka, S., Aremu, D.A. 2008. ^{13}C heteronuclear NMR studies of the interaction of cultured neurons and astrocytes and aluminum blockade of the preferential release of citrate from astrocytes. *J Biol Inorg Chem.* 13, 241-247.

Nayak, P. 2002. Aluminum: impacts and disease. *Environ Res.* 89, 101-115.

Nayak, P., Chatterjee, A.K. 2002. Response of regional brain glutamate transaminases of rat to aluminum in protein malnutrition. *BMC Neurosci.* 28; 3:12.

Perl, D.P., Brody, A.R. 1980. Alzheimer's disease: X-ray spectrometric evidence of aluminum accumulation in neurofibrillary tangle-bearing neurons.

Perl, D.P., Moalem, S. 2006. Aluminum and Alzheimer's disease, a personal perspective after 25 years. *J Alzheimers Dis.* 9, 291-300.

Platt, B., Fiddler, G., Riedel, G., Henderson, Z. 2001. Aluminium toxicity in the rat brain: histochemical and immunocytochemical evidence. *Brain Res Bull.* 55, 257-267.

Poliandri, A.H., Cabilla, J.P., Velardez, M.O., Bodo, C.C., Duvilanski, B.H. 2003. Cadmium induces apoptosis in anterior pituitary cells that can be reversed by treatment with antioxidants. *Toxicol Appl Pharmacol.* 190, 17-24.

Poliandri, A.H., Machiavelli, L.I., Quinteros, A.F., Cabilla, J.P., Duvilanski, B.H. 2006. Nitric oxide protects the mitochondria of anterior pituitary cells and prevents cadmium-induced cell death by reducing oxidative stress. *Free Radic Biol Med.* 40, 679-688.

Priest, N.D. 204. The biological behaviour and bioavailability of aluminium in man, with special reference to studies employing aluminium-26 as a tracer: review and study update. *J Environ Monit.* 6, 375-403.

Quinteros, F.A., Machiavelli, L.I., Miler, E.A., Cabilla, J.P., Duvilanski, B.H. 2008. Mechanisms of chromium (VI)-induced apoptosis in anterior pituitary cells. *Toxicology.* 249, 109-115.

Quinteros, F.A., Poliandri, A.H., Machiavelli, L.I., Cabilla, J.P., Duvilanski, B.H. 2007. In vivo and in vitro effects of chromium VI on anterior pituitary hormone release and cell viability. *Toxicol Appl Pharmacol.* 218, 79-87.

Roberts, N.B., Clough, A., Bellia, J.P., Kim, J.Y., 1998. Increased absorption of aluminium from a normal dietary intake in dementia. *J. Inorg. Biochem.* 69, 171-176.

Salzman, G.C., Crowell, J.M., Martin, J.C., Trujillo, T.T., Romero, A., Mullaney, P.F., LaBauve, P.M. 1975. Cell classification by laser light scattering: identification and separation of unstained leukocytes. *Acta Cytol.* 19, 374-377.

Sánchez-Iglesias, S., Soto-Otero, R., Iglesias-González, J., Barciela-Alonso, M.C., Bermejo-Barrera, P., Méndez-Alvarez, E. 2007. Analysis of brain regional distribution of aluminium in rats via oral and intraperitoneal administration. *J Trace Elem Med Biol.* 21, 31-34.

Sargazi, M., Roberts, N.B., Shenkin, A. 2001. In-vitro studies of aluminium-induced toxicity on kidney proximal tubular cells. *J Inorg Biochem.* 87, 37-43.

Savory, J., Ghribi, O., Forbes, M.S., Herman, M.M. 2001. Aluminium and neuronal cell injury: inter-relationships between neurofilamentous arrays and apoptosis. *J Inorg Biochem.* 87, 15-19.

Savory, J., Herman, M.M., Ghribi, O. 2003. Intracellular mechanisms underlying aluminum-induced apoptosis in rabbit brain. *J. Inorg. Biochem.* 97, 151–154.
Science. 208, 297-299.

Stojilkovic, S.S. 2006. Pituitary cell type-specific electrical activity, calcium signaling and secretion. *Biol Res.* 39, 403-423.

Suárez-Fernández M.B., Soldado, A.B., Sanz-Medel, A., Vega, J.A., Novelli, A., Fernandez-Sanchez, M.T. 1999. Aluminum-induced degeneration of astrocytes occurs via apoptosis and results in neuronal death. *Brain Research.* 835, 125–136.

Toimela, T., Tahti, H. 2004. Mitochondrial viability and apoptosis induced by aluminum, mercuric mercury and methylmercury in cell lines of neural origin. *Arch Toxicol.* 78, 565–574

Walton, J.R. 2004. A bright field/fluorescent stain for aluminum: its specificity, validation, and staining characteristics. *Biotech Histochem.* 79, 169-176.

Yokel, R.A. 2002. Brain uptake, retention, and efflux of aluminum and manganese. *Environ Health Perspect.* 110, 699-704.

Yokel, R.A. 2006. Blood-brain barrier flux of aluminum, manganese, iron and other metals suspected to contribute to metal-induced neurodegeneration. *J Alzheimers Dis.* 10, 223-253.

Yumoto, S. Nagai, H. Matsuzaki, H. Matsumura, H. Tada, W. Nagatsuma, E. Kobayashi K. 2001. Aluminium incorporation into the brain of rat fetuses and sucklings. *Brain Res Bull.* 55, 229-234.

Zatta, P., Favarato, M., Nicolini, M. 1993. Deposition of aluminium in brain tissues of rats exposed to inhalation of aluminium acetylacetonate. *NeuroReport.* 4, 1119–1122

Zhang, Q.L., Boscolo, P., Niu, P.Y., Wang, F., Shi, Y.T., Zhang, L., Wang, L.P., Wang, J., Di Gioacchino, M., Conti, P., Li, Q.Y., Niu, Q. 2008. How do rat cortical cells cultured with aluminum die: necrosis or apoptosis? *Int J Immunopathol Pharmacol.* 21, 107-115.

II. Aluminium effect in elementary exocytotic events of rat pituitary lactotroph-enriched culture

1. Introduction

The growing industrial interest in aluminium and its compounds for manifold purposes has been accompanied by an ascending concern about the toxic potential of aluminium. Whilst it is well recognized the aluminium neurotoxicity in experimental animals (Kopeloff *et al.*, 1950; Erasmus *et al.*, 1993) and in individuals with renal failure (Sweeney *et al.*, 1985; Fernández-Martín *et al.*, 2000; Zatta *et al.*, 2004), the adverse health effects of occupational exposure and linked with daily routine remain elusive.

Decreased concentrations of prolactin in serum have been reported in a five years epidemiological study involving 227 subjects with occupational exposure to aluminium (Alessio *et al.*, 1989). Prolactin has a broad spectrum of activities at the level of reproduction, metabolism, osmoregulation, immunoregulation and behaviour (see review Bole-Feysot *et al.*, 1998). Despite extrapituitary sites also contributes to derive prolactin in humans, the main source of serum prolactin are lactotrophs, which comprise 20-50% of total anterior pituitary cells (Turgeon *et al.*, 2001). The secretory activity of the lactotrophs mirrors the action of a complex network of local and distant regulators (Freeman *et al.*, 2000), orchestrated by hypothalamus which tonically suppresses prolactin secretion from the pituitary (Angleson *et al.*, 1999; Freeman *et al.*, 2000). Thereby, alterations of plasma prolactin levels are often interpreted as resulting from an impaired hypothalamic dopaminergic modulation of pituitary secretion, given that hypothalamic dopamine released into the hypophysial portal systems is the major prolactin-inhibiting factor (MacLeod and Lehmeyer, 1974; Ben-Jonathan and Hnasko, 2001). At a first glance, the reported decrease of serum prolactin levels after exposure to aluminium suggests exacerbated hypothalamic delivery of dopamine, which seems not to be the case. *In vivo* exposure to aluminium produces a diminishment of the levels of dopamine, dihydroxyphenylacetic acid and homovanillic acid in mice hypothalamus consistent with aluminium-induced inhibition of dopamine synthesis (Tsunoda and Sharma, 1999). Aluminium seems also to have a pronounced activatory effect on the amine oxidases, MAO-A and MAO-B, which catalyse the oxidative deamination of dopamine (Zatta *et al.*, 1998).

Recently, a new sensitive bright field/fluorescent histochemical staining method, based on phloxine B and phosphotungstic acid, with ethanol differentiation has been developed by Walton (2004). This method allows specific detection of aluminium in tissue sections with subcellular resolution. It was clearly demonstrated that aluminium accumulation in the cytoplasm of some cells of the anterior pituitary occurs, since it was

detected in tissue sections obtained from a 24 month old male Wistar rat previously gavaged with 8 mg of aluminium (aluminum sulfate in citrus juice) at 2, 4, 5, 7, and 13 months of age. A comparative analysis of the aluminium concentrations in different organs following twice a day administration of aluminium citrate (2 ng Ag per g of diet) during one month through ruminal cannulas to wether lambs has been conducted (Allen *et al.*, 1991). A more prominent increment of the aluminium concentration in the pituitary gland than in the brain has been observed. Furthermore, control animals also showed higher concentrations of aluminium in the pituitary gland than in the brain, suggesting that pituitary cells could be challenged by aluminium even primary to aluminium-induced impairment of hypothalamic dopaminergic modulation of pituitary secretion of prolactin.

Lactotrophs are distinctive by having an intrinsic capacity for high production and secretion of prolactin (Ben-Jonathan and Hnasko, 2001). When in culture, lactotrophs exhibit spontaneous and stimulated exocytosis of peptidergic vesicles (Angleton *et al.*, 1999; Vardjan *et al.*, 2007a). For that reason, lactotroph-enriched cell cultures are the right choice to study pituitary secretion of prolactin not under neuroendocrine control. Moreover, it has been extensively demonstrated that multiple mechanisms of exocytosis can be solved in single lactotroph experiments addressing elementary properties of the interaction between a single vesicle and the plasma membrane (Angleton *et al.*, 1999; Stenovec *et al.*, 2004; Lledo *et al.*, 1993; Vardjan *et al.*, 2007a). In spite of being intrinsically related processes, prolactin secretion (the cargo delivery from the peptidergic vesicles to the extracellular space) and exocytosis, which leads to the formation of an aqueous fusion pore between the peptidergic vesicle and the plasma membrane, should be considered as independent events. Prolactin secretion can occur when prolactin-containing vesicles merge with the plasma membrane completely in consequence of the expansion of the fusion pore (full fusion exocytosis) (Angleton *et al.*, 1999; Chowdhury *et al.*, 2006; Vardjan *et al.*, 2007a) and when its reversible closure occurs only after a phase of pore expansion, well-suited to allow cargo release from prolactin-containing vesicles, followed either by reversible fusion ("kiss-and-run" exocytosis) (Stenovec *et al.*, 2004; Vardjan *et al.*, 2007a) or stable, long-lasting, regular fusion pore gating (pulsing pore exocytosis) (Stenovec *et al.*, 2004; Vardjan *et al.*, 2007a). Otherwise release-unproductive exocytosis takes place, it means that the fusion of peptidergic vesicle with the plasma membrane is not accompanied by secretion of prolactin (Vardjan *et al.*, 2007a; Vardjan *et al.*, 2007b). Real time studies showed that peptidergic vesicle exocytosis is mainly refereed a regulated, Ca²⁺-dependent membrane fusion event with distinct kinetic pathways controlled by intracellular signalling cascades, protein-protein and lipid-protein

interactions at the level of vesicle and plasma membranes (Angleton *et al.*, 1999; Chowdhury *et al.*, 2006). Thereby, aluminium has a myriad of opportunities for interfering with fusion pore properties, which can be considered the last regulated step of prolactin secretion by lactotrophs.

In the past, aluminium-induced alterations of membrane physical properties, like modification of membrane fluidity or membrane lipid composition, have been extensively reported (Zubenko, 1990; Ohba *et al.*, 1994; Sarin *et al.*, 1997; Silva *et al.*, 2002; Verstraeten and Oteiza, 2002; Pandya *et al.*, 2004), which are expected to ground abnormal functioning of membrane fusion processes (Zimmerberg and Chernomordik 1999; Kozlovsky 2002; Churchward *et al.*, 2008).

The leading role of the phosphatidylinositol 4,5-bisphosphate (PIP₂) binding protein CAPS (Ca²⁺-dependent activator protein for secretion) in determining the kinetics of regulated exocytosis have been highlighted and contested (Loyet *et al.*, 1998; Grishanin *et al.*, 2004). The inhibition of PIP₂-specific phospholipase C by aluminium (Shi *et al.*, 1993; Shafer and Mundy, 1995; Nostrandt *et al.*, 1996) places aluminium again in the core of the regulatory mechanisms of the Ca²⁺-dependent membrane fusion. In addition to the above mentioned aluminium-induced impairment of the phosphoinositide second messenger-producing system, many experimental evidences support the interference of aluminium with signaling cascades involving G proteins (Kanaho *et al.*, 1985; Provan and Yokel, 1992; Haug *et al.*, 1994), cyclic AMP (Ebstein *et al.*, 1986) and calcium (Siegel and Haug, 1983; Provan and Yokel, 1992; Julka and Gill, 1996), which have been often implicated in the still largely unknown mechanisms of regulated exocytosis (review in Seino and Shibasaki, 2005).

While the lipid/protein machinery and the microenvironmental constrains of the multiple molecular mechanisms of exocytosis remain to be deeply integrated to give a mechanistic interpretation to the process, this work was simply undertaken with the specific aim of determining whether exposure to aluminium of rat anterior pituitary cells induces alterations of the fusion pore properties consistent with a depressed secretion of prolactin by pituitary lactotrophs. In order to reach this goal, a cell-attached patch clamp technique was used to study elementary fusion pore properties by electrophysiological membrane capacitance measurements. Discrete changes in membrane capacitance of membrane patches were monitored prior and post stimulation of rat pituitary lactotroph-enriched cell cultures, which viability remained unchanged after exposed to AlCl₃ during 24 h.

2. Materials and methods

2.1. Cell culture and aluminium exposure

Male Wistar rats were handled in accordance with guidelines for the accommodation and care of animals used for experimental and other scientific purposes the guidelines for the care and use of experimental animals (Official Journal of the European Union L197 of 30.7.2007). Primary cultures were obtained from the anterior pituitaries as described previously (Ben-Tabou *et al.*, 1994). The rat pituitary lactotroph-enriched cultures, maintained either in suspension or plated on poly-L-lysine coated glass coverslips, were stored at 37°C, 92% humidity and 5% CO₂ in high-glucose DMEM buffered with HEPES-Tricine and supplemented with 1.5 µM BSA, 2 mM L-glutamine and 1% newborn calf serum. Incubation medium was changed every second day and experiments were carried out at room temperature 1 to 4 days after the isolation. 24-Hour aluminium exposure was initiated by addition of AlCl₃ (final concentration 30 µM) to the incubation medium and the cell cultures were maintained under the above mentioned conditions.

2.2. Electrophysiology

Cell-loaded coverslips were placed in a recording chamber on the inverted microscope (Zeiss AXIO Observer, Jena, Germany) and supplied with extracellular solution (10 mM D-glucose, 130 mM NaCl, 8 mM CaCl₂, 1 mM MgCl₂, 5 mM KCl, buffered at pH 7.2 with 10 mM HEPES and NaOH). The micropipette was also filled with extracellular solution and with the help of a micromanipulator, the tip was approached to the plasma membrane of a single cell. To perform electrophysiological membrane capacitance measurements under stimulation conditions, 130 mM KCl, 5 mM NaCl, 8 mM CaCl₂, 1 mM MgCl₂, 10 mM D-glucose and 10 mM HEPES/NaOH (pH 7.4) was drop into the recording chamber to reach the final concentration of 100 mM KCl.

Cell-attached capacitance measurements were performed with a dual-phase lock-in patch-clamp amplifier (sine-wave frequency (f) 1591 Hz; 111 mV root mean square; SWAM IIC, Celica, Ljubljana, Slovenia). A sine wave voltage was applied to the pipette and the pipette potential was set at 0 mV. The patch pipette resistance ranged from 3 to 6 MΩ. Phase angle was adjusted to nullify the changes in the real (R_e) trace. 10 fF calibration pulses in the imaginary part (I_m) of admittance were manually generated every

10 s to guarantee correct phase angle settings, as previously described (Kreft and Zorec, 1997; Sikdar *et al.*, 1998). For transient fusion events, vesicle capacitance (C_v) and fusion-pore conductance (G_p) were calculated from the I_m and R_e part of admittance signals as reported previously (Lollike and Lindau, 1999):

$$G_p = (R_e^2 + I_m^2)/R_e; C_v = [(R_e^2 + I_m^2)/I_m]/\omega$$

where ω is the angular frequency ($\omega = 2\pi f$).

Fusion pore radius was estimated by using the following equation:

$$G_p = (\pi r^2)/(\rho \lambda)$$

where r denotes fusion pore radius, ρ the estimated resistivity of the saline (100 Ω cm), and λ the estimated length of a gap junction channel (15 nm) (Spruce *et al.*, 1990). Vesicle diameter was calculated by using specific membrane capacitance of 8 F/ μm^2 . Transient events were analyzed in the home-made software (CellAn, Celica, Slovenia) written for MATLAB (Math Works, Natick, MA, USA) on PC computers.

2.3. Data analysis

All results are presented as mean \pm SEM of the number of experiments indicated in the legends of the figures. Statistical significance was evaluated by Student's t-test and p values are presented in the figures

3. Results and Discussion

3.1. Capacitance measurements of spontaneous fusion events after exposure to AlCl_3

The rat pituitary lactotrophs-enriched culture used in this work is a well-characterised prolactin-secreting cell culture in which large dense-core vesicles (mean diameter of 250 nm) undergo Ca^{2+} -regulated exocytosis and their ensuing endocytic retrieval (Smets *et al.*, 1987; Bauer *et al.*, 2004; Stojilkovic, 2005) while constitutive endo- and exocytosis are thought to involve much smaller vesicles (mean diameter under 100 nm) (Pow and Morris, 1991; Senda *et al.*, 1991; Haass *et al.*, 1996). Both processes alter the cell surface area in discrete steps that can be monitored by cell-attached patch-clamp measurements of membrane capacitance (C_m) in resting and stimulated cells (Angleton and Betz, 1997; Klyachko and Jackson, 2002). It has been noticeably demonstrated that when lactotrophs are stimulated the most prominent alteration impacting discrete C_m changes is the engagement of large dense-core vesicles in “kiss-and-run” mode of exocytosis (Vardjan *et al.*, 2007). Hence we performed electrophysiological C_m measurements in cell-attached patch-clamp configuration to study sublethal effects of AlCl_3 on large dense-core vesicle fusion/fission with the plasma membrane of lactotrophs. After exposure of rat pituitary lactotrophs-enriched cultures to 30 μM AlCl_3 during 24 h, the incubation medium was replaced by a Ca^{2+} -enriched saline solution devoided of any added aluminium and C_m measurements were performed in 12 patches. Epochs of representative I_m (imaginary component reflecting patch capacitance) and R_e (real component reflecting patch conductance) traces are shown in Fig. 1 to illustrate the recorded types of discrete steps in C_m . Occasionally, the rapid onset of long-lasting changes of the I_m signal has been observed in both directions (Fig. 1, A and B). These types of discrete steps in C_m were interpreted as representing full fusion (irreversible upward steps) and endocytotic retrieval (irreversible downward steps) of large dense-core vesicles, accordingly to exhaustive studies performed with rat pituitary lactotrophs-enriched cultures (Stenovec *et al.*, 2004; Chowdhury *et al.*, 2006; Vardjan *et al.*, 2007a). In general, upward steps in I_m trace were followed by a downward step of similar magnitude within few seconds (Fig. 1C). These reversible events often exhibited significant cross talk between I_m and R_e signals (Fig. 1C). From time to time event bursts emerged (Fig. 1C) or up- downward steps exhibited more complex shapes (data not shown), consistent with multiple vesicle fusion/fission (Cochilla *et al.*, 2000; Pickett and

Edwardson, 2006). These types of discrete steps in C_m of the patches against time (Fig. 1C) most likely resulted from fusion (upward steps) and fission (downward steps) events involving large dense-core vesicles and the plasma membrane. Actually, the amplitude of all observed reversible steps in C_m ranged from 0.29 fF to 5.34 fF, which could be justified by “kiss-and-run” of vesicles with diameters from 101 nm to 434 nm, as previously demonstrated (Smets *et al.*, 1987; Vardjan *et al.*, 2007a).

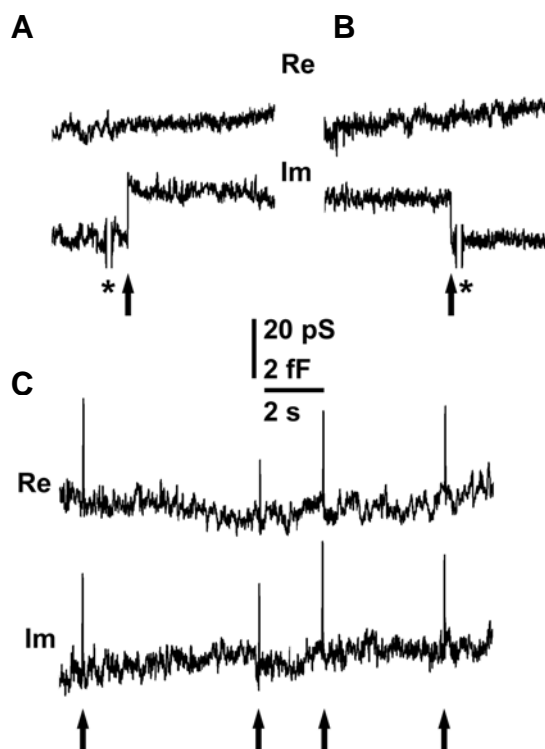


Figure 1. Spontaneous fusion and fission events in cell-attached patches of cells previously exposed to aluminium.

The epochs of I_m and R_e traces show representative discrete steps monitored in C_m (arrows) of 10 patches during spontaneous conditions. Changes of the I_m signal lasting for more than 5 s were considered irreversible steps reflecting an increase (A) or a decrease (B) in C_m . The I_m steps were recurrently reversible either exhibiting significant cross talk with the R_e signal (C). Asterisks denote calibration pulses (10 fF) that do not project to the R_e signal, indicating correct phase angle setting of the lock-in amplifier.

Fig. 2 shows a Gaussian distribution of transient capacitance fusion events from all the recordings performed with cells previously exposed to $AlCl_3$. The mean amplitude of these single spontaneous events was 1.87 ± 0.12 fF ($n = 134$), suggesting that the studied vesicles exhibited an average diameter of 257 ± 15 nm, matching that of prolactin-containing vesicles (Smets *et al.*, 1987; Angleson *et al.*, 1999; Vardjan *et al.*, 2007). So, in cells previously exposed to $AlCl_3$, it was possible to observe all types of discrete steps in

C_m involving large dense-core vesicles, which have been depicted before in lactotrophs (Stenovec *et al.*, 2004; Chowdhury *et al.*, 2007; Vardjan *et al.*, 2007a).

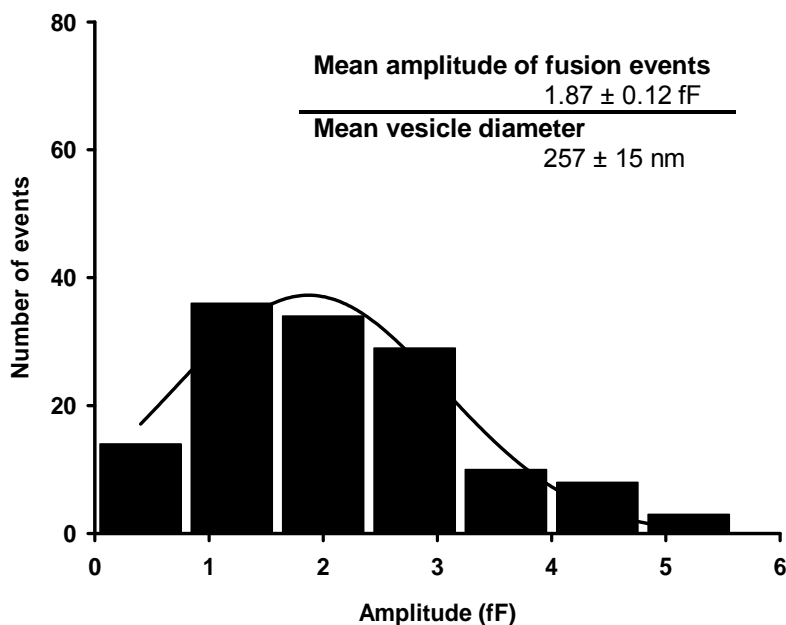


Figure 2. Amplitude of reversible capacitance fusion events in cell-attached patches of cells previously exposed to aluminium.

The histogram represents the distribution of amplitudes of C_v recording during reversible fusion pore events ($n = 134$) under spontaneous conditions. The curve shows a fitted Gaussian distribution ($R^2 = 0.94$) to the data with mean \pm SEM values displayed as insert.

3.2. Frequency of stimulated fusion events after exposure to $AlCl_3$

After recording the spontaneous activity of cells previously exposed to $AlCl_3$ as mentioned above, a K^+ -depolarising stimulus has been applied in the absence of added aluminium (see “Material and methods”) and recording of the stimulated activity proceed during several minutes. In 4 of the 10 patches, it was only possible to monitor discrete steps in C_m before stimulation. Discrete steps in C_m before and after stimulation were successfully measured in the other 6 patches. We observed that out of 109 events, 91 events took place before stimulation (total recording time of 3129 s) and only 18 events occurred after stimulation (total recording time 3377 s). These results suggest that cells previously exposed to $AlCl_3$ failed to respond to K^+ -depolarising stimulus by increasing the frequency of fusion/fission events.

Table I presents the effect of stimulation on the frequency of fusion and fission events as revealed in the 6 patches that exhibited both activities, spontaneous and

stimulated. After stimulation the frequency of reversible events decreased significantly ($p < 0.01$) from 0.022 ± 0.005 events/s ($n = 82$ events) to 0.005 ± 0.001 events/s ($n = 13$ events). The irreversible events accounted for only a minor fraction ($\sim 13\%$) of the total 109 events observed, rendering impossible any strictly comparative analysis of their frequency before and after stimulation. The incidence of irreversible upward steps was 0.002 ± 0.001 events/s and 0.0006 ± 0.0004 events/s before and after stimulation, respectively. Apparently, the occurrence of irreversible downward steps remained almost unchanged (0.0006 ± 0.0004 events/s and 0.0008 ± 0.0006 events/s, before and after stimulation, respectively).

Table I. Effect of stimulation on the frequency of fusion and fission events in cells previously exposed to aluminium

Condition	Discrete steps in C_m (events/s)		
	Reversible	Irreversible	
		Upward	Downward
Before stimulation (3129 s)	0.022 ± 0.005 ($n = 82$)	0.002 ± 0.001 ($n = 7$)	0.0006 ± 0.0004 ($n = 2$)
Upon stimulation (3377 s)	0.005 ± 0.001 *** ($n = 13$)	0.0006 ± 0.0004 ($n = 2$)	0.0008 ± 0.0006 ($n = 3$)

Frequency values are given in mean \pm SEM, the total recording time and the total number of events being given in parentheses.

*** $p < 0.01$ as compared to event frequency before stimulation by t -test.

These results are in line with those reported by Vardjan *et al.*, (2007a), showing the reversible character of the majority of fusion events prior and upon K^+ -induced depolarization of lactotrophs not exposed to aluminium. In contrast to the above mentioned study, we observed a reduction rather than an enhancement of “kiss-and-run” mode of exocytosis in response to stimulation. Actually, our results clearly show that rat pituitary lactotrophs-enriched cultures, after 24h-exposure to $30 \mu\text{M AlCl}_3$, do not respond to stimulation with high K^+ concentration by increasing the frequency of transient C_m changes, which correspond to the “kiss-and-run” mode of exocytosis.

To determine whether aluminium, acting as a fusion promoter, could render impossible extra increment of the frequency of fusion events upon stimulation, we performed an additional set of experiments using cells from the same batch of rat pituitary lactotrophs-enriched culture but not previously exposed to aluminium. Spontaneous fusion and fission events, appearing as reversible and irreversible (up- and downward) steps in C_m measurements, were observed in 36 % of 22 analysed patches. Thereby, we recorded I_m and R_e signals in 8 patches with a total recording time of 4647 s. During the period of observation, a total number of 160 events have been recorded. We verified that reversible

steps on C_m traces account for the major fraction (79 %) of the total number of observed events. This value is consistent with previous reported contribution of “kiss-and-run” to spontaneous exocytotic activity of lactotrophs (Vardjan *et al.*, 2007a). As can be observed in Table II, exposure to $AlCl_3$ did not cause significant changes in the frequency of discrete steps in C_m measurements under spontaneous conditions, supporting that aluminium does not promote fusion of large dense-core vesicles with the plasma membrane.

Table II. Spontaneous frequency of fusion and fission events in cells that have either been exposed or not exposed to aluminium

Condition	Discrete steps in C_m (events/s)		
	Reversible	Irreversible	
		Upward	Downward
No exposure (4647 s)	0.027 ± 0.005 (n = 127)	0.0044 ± 0.0014 (n = 20)	0.0029 ± 0.0009 (n = 13)
After exposure (5580 s)	0.027 ± 0.005 (n = 150)	0.0021 ± 0.0006 (n = 12)	0.0007 ± 0.0003 *

Frequency values are given in mean ± SEM, the total recording time and the total number of events being given in parentheses.

* $p < 0.05$ as compared to event frequency before stimulation by t -test.

3.3. $AlCl_3$ effect on the profile of “kiss-and-run” fusion events

Although under resting conditions no significant differences could be observed in the frequency of transient capacitance fusion events due to exposure to $AlCl_3$, the fraction of events exhibiting discernible cross talk between the I_m and R_e parts of the admittance signals was noticeably enhanced by aluminium (Fig. 3A). These cross talks were revealed in 37 ± 14 % (39 out of 110) of the transient capacitance fusion events that occurred in cells not previously exposed to $AlCl_3$, whereas this percentage reached 74 ± 11 % (124 out of 134) after exposure to $AlCl_3$. Remarkably, cross talks were detected in 12 out of 13 reversible events that took place upon stimulation of cells previously exposed to $AlCl_3$. It is important to note that each reported transient capacitance change very likely reflects a single fusion event. In fact, Fig. 3 (panel B) reveals a high correlation ($R^2 = 0.96$) between the upward step and the correspondent downward step within a transient capacitance event when fitted by linear regression ($slope = 0.94 \pm 0.07$; $n = 257$) under all studied conditions. The existence of discernible cross talk between the I_m and R_e parts of the admittance signals during “kiss-and-run” in lactotrophs is currently interpreted as reflecting transient formation of fusion pores with low conductance (narrow fusion pores) (Spruce *et al.* 1990; Vardjan *et al.*, 2007a). Under our recording conditions, measurable pore conductance (G_p) values ranged from 5 pS to 236 pS, which correspond to fusion pore

diameters of 0.3 – 2.1 nm. Despite that “kiss-and-run” fusion seems to proceed in rat pituitary lactotrophs-enriched cultures under our conditions of exposure to aluminium, it is uncertain that prolactin secretion would occur. On the contrary, evidence that productive secretion might not take place is supported by the fact that our results clearly showed that the majority of fusion pores exhibited diameters below 2.1 nm whereas 5 nm is thought to be the minimal value of fusion pore diameter required for release of prolactin from vesicular lumen to the extracellular space (Vardjan *et al.*, 2007a). These results, obtained with rat pituitary lactotrophs-enriched cultures, confirm the aluminium-induced transition from productive to unproductive mode of exocytosis previously revealed by single-cell electrophysiological studies (Fig. 3).

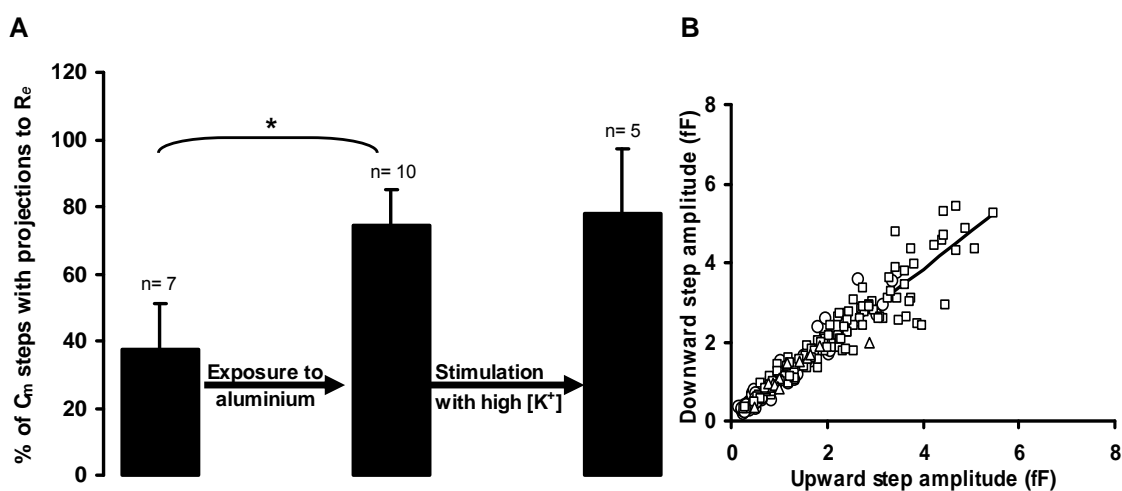


Figure 3. Effect of exposure to aluminium on the incidence of reversible conductance changes at the time of capacitance steps reflecting single large dense-core vesicle fusion events.

The stepwise capacitance increases, consistent with fusion of single large dense-core vesicles with the plasma membrane (0.29 – 5.34 fF), were analysed during spontaneous conditions and following stimulation with 100 mM K^+ . The percentage of events that revealed simultaneous changes of the two measured lock-in outputs I_m and R_e (see Fig. 1C) is presented in panel A. Values are given as the mean \pm SEM of the number of events indicated above bars. Statistical significance $*p < 0.05$, compared to the respective control. Panel B shows that the amplitudes of the upward and ensuing downward capacitance steps are directly proportional to one another (best-fit straight line $y = 0.94x$; $R^2 = 0.96$) in all analysed events ($n = 257$). Spontaneous events in cells that have either been not exposed (\circ) or exposed to 30 μM $AlCl_3$ before (Δ) and after stimulation (\square).

3.4. $AlCl_3$ effect on fusion pore properties

To depict the huge aluminium-induced width reduction of fusion pores, we further contrast other parameters of “kiss-and-run” events using cells from the same batch of rat

pituitary lactotrophs-enriched cultures that have either been exposed or not exposed to AlCl_3 .

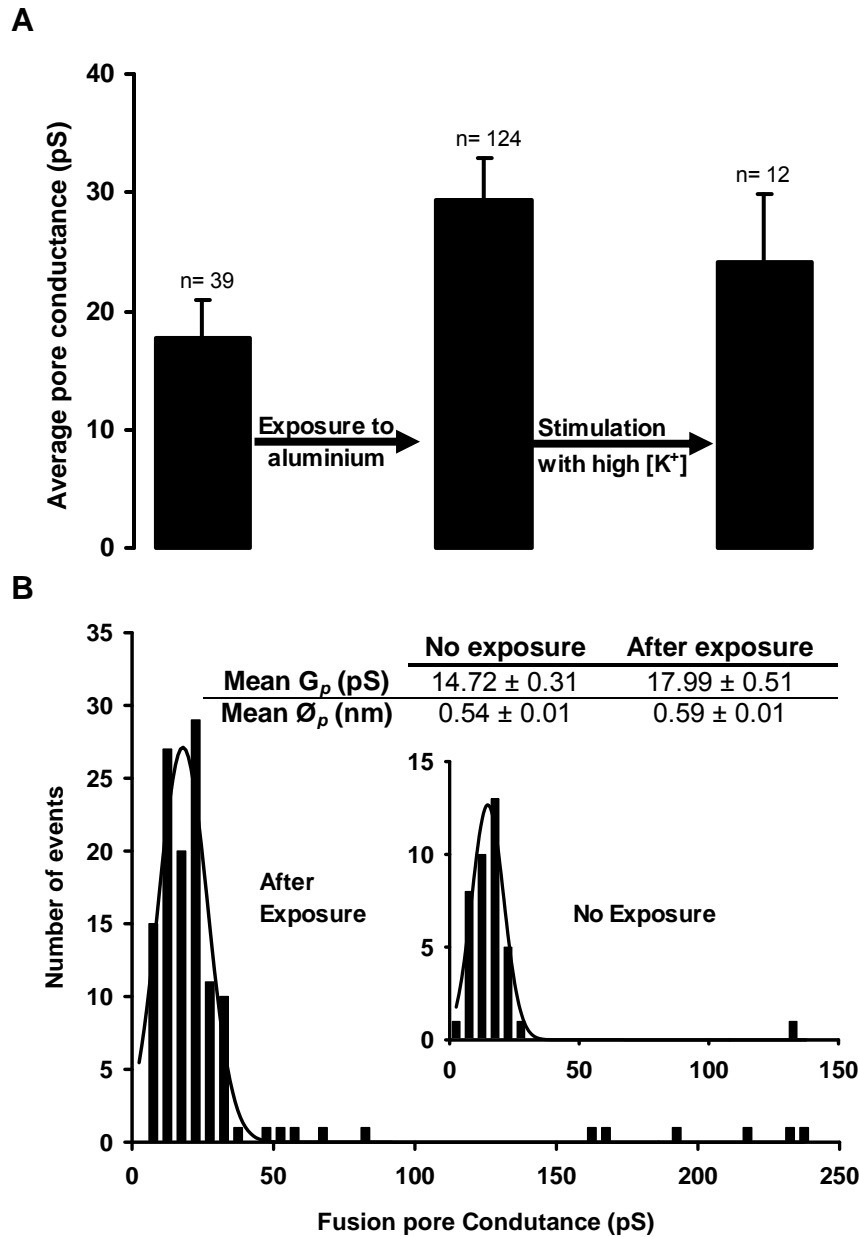


Figure 4. Effect of exposure to aluminium on fusion pore conductance within the range of resolution for G_p measurements.

The G_p values of all fusion events that revealed simultaneous changes of the two measured lock-in outputs I_m and R_e analysed in Fig. 3 ($n = 175$) have been calculated for spontaneous events in cells that have either been not exposed or exposed to $30 \mu\text{M AlCl}_3$ before and after stimulation with 100 mM K^+ . The aluminium-induced effects on the average G_p values and on the distribution of conductance of fusion events are displayed in panel A and B, respectively. Average values are given as the mean \pm SEM of the number of events indicated above bars. The curves shows a fitted Gaussian distribution ($R^2 = 0.92$ and 0.96) to the data with mean \pm SEM values displayed as insert.

As already mentioned above, discernable cross talks between the I_m and R_e parts of the admittance signals were often observed during transient capacitance fusion events under our experimental conditions, which raised the opportunity to address the question whether exposure to $AlCl_3$ alters measurable G_p values (Fig. 4).

Surprisingly, after exposure to $AlCl_3$ the average values of G_p (resting conditions: 29 ± 4 pS, $n = 124$; stimulating conditions: 24 ± 6 pS, $n = 12$) were higher than 18 ± 3 pS ($n = 39$), which corresponds to the average value of G_p determined in patches of cells not previously exposed to aluminium.

This effect was mainly due to the aluminium-induced increase of relative incidence of fusion pores exhibiting G_p values in the range of 7 to 236 pS rather than to significant alteration of the mean peak of measurable fusion pore conductance (Fig. 4B). Taking into consideration that these results reflect only the properties of narrow fusion pores (transient capacitance fusion events exhibiting discernable cross talks between the I_m and R_e parts of the admittance signals), most likely exposure to aluminium deterred further enlargement of fusion pores. In fact, more fusion events with measurable G_p were observed (Fig. 3A) and 20 out of 124 (16 %) exhibited G_p values larger than that of the majority (97 %) of events observed in cells not previously exposed to $AlCl_3$ (Fig. 4B). However, more fusion events with measurable G_p were observed after exposure of rat pituitary lactotrophs-enriched cultures to aluminium (Fig. 3A) and stimulation did not increase G_p values (Fig. 4A). These observations led to suggest that most likely exposure to aluminium deterred rapid expansion of fusion pores. As it can be observed in Fig. 5, exposure to aluminium induced a shift toward low values of G_p of reversible events mediated by fusion pores found to remain with a conductance below 35 pS. In contrast, no significant differences have been observed between the mean dwell-time of fusion pores with low conductance from all the recordings performed with cells from the same batch of rat pituitary lactotrophs-enriched cultures that have either been exposed (0.053 ± 0.003 s) or not exposed to $AlCl_3$ (0.059 ± 0.001 s), which values lied within the natural range of fluctuation of this parameter for spontaneous transient fusion events (Stenovec *et al.*, 2004; Vardjan *et al.*, 2007a). Meanwhile, cells previously exposed to aluminium seem to respond to K^+ -depolarising stimulus by increasing fusion pore dwell-time significantly (Fig. 5, inserts), as previously depicted for lactotrophs not exposed to aluminium (Vardjan *et al.*, 2007a). Yet it could be argued that after exposure to aluminium the average conductance of relatively fewer stimulated fusion events was apparently larger than that of resting values exhibiting the same amplitude (Fig. 5), data displayed in and Fig. 3 quarrel over

fusion pore expansion during prolongation of residing time of a single vesicle connected with the extracellular space in response to stimulation.

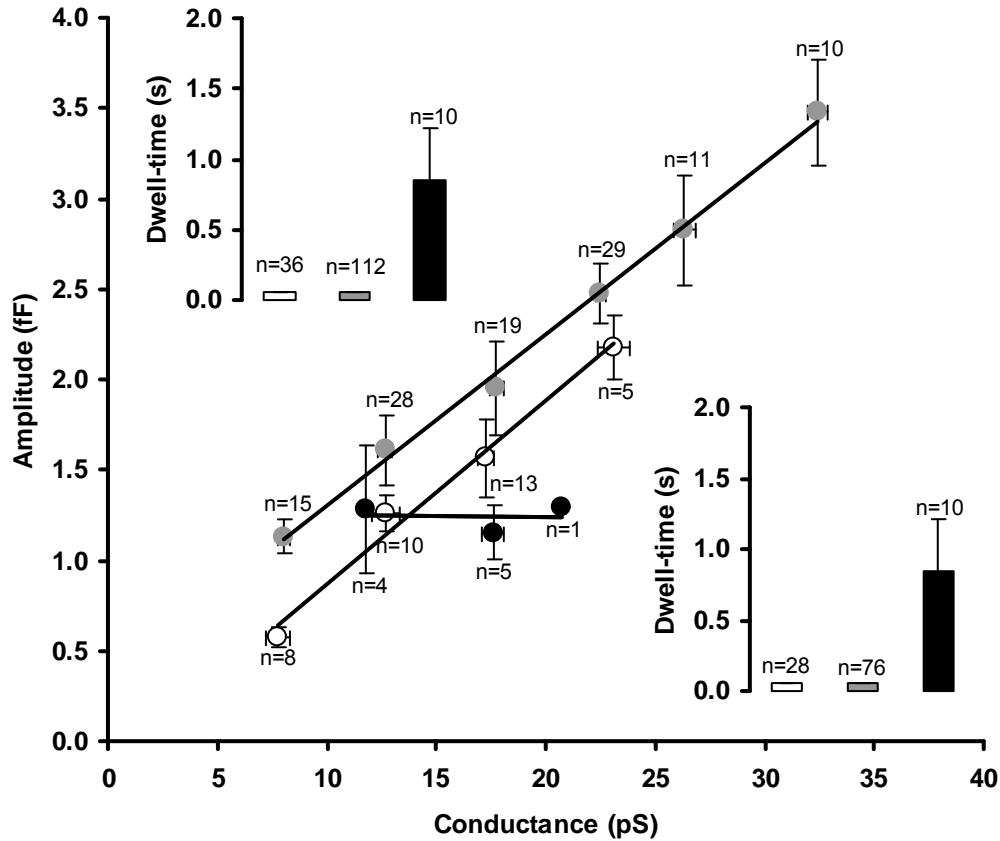


Figure 5. Effect of exposure to aluminium on dwell-time and amplitude of reversible fusion events mediated by fusion pores with low conductance.

The average values of G_p and C_v of events with conductance smaller than 35 pS were calculated after splitting the range of the data in 5 pS conductance classes, which correspond to the most frequent classes of the conductance histograms displayed in Fig. 4B. Average values are given as the mean \pm SEM of the number of events indicated above each data point in the scatter graph. In addition to spontaneous events in cells that have either been not exposed (white symbols) or exposed to 30 μ M AlCl₃ (grey symbols), the relatively fewer events occurring after stimulation with 100 mM K⁺ events were also analysed in a similar manner and their average values of G_p and C_v plotted (black symbols). The dwell-time of the analysed events under the different conditions are contrasted either considering all the analysed fusion events (top insert) or only the subset of events that correspond to G_p and C_v closely matching that of stimulated events (from 10 to 25 pS) (bottom insert). Average values are given as the mean \pm SEM of the best fitted Gaussian curves ($R^2 = 0.65$ and 0.88) for spontaneous conditions and single-exponential curve ($R^2 = 0.85$) for stimulating condition.

We used patch clamp cell-attached technique on single cells to show for the first time how aluminium affects elementary regulated exocytotic events and their fusion pore properties. Data derived from neuroendocrine cells can often be extrapolated in predicting effects in neurons and vice versa (Neher, 1998), since the molecular machinery participating in Ca^{2+} -regulated exocytosis shows great similarities. Therefore, the aluminium-induced switch to unproductive exocytosis depicted in rat pituitary lactotrophs-enriched cultures might contribute to explain how this neurotoxic agent alters neurotransmitter release. Besides studies concerned with aluminium effect on the release of neurotransmitters still very limited (see review in Gonçalves and Silva, 2007), there is some evidence that has already come forward to show aluminium-induced inhibition of neurotransmitter release. For instance, Ca^{2+} -dependent, K^+ depolarization triggered release of acetylcholine and glutamate release is highly diminished after exposure to AlCl_3 (Szutowicz *et al.*, 1998; Jankowska *et al.*, 2000; Silva *et al.*, 2007), which is consistent with unproductive exocytosis.

Although the exact mechanism underlying the aluminium effect on exocytotic events was not completely elucidated, our results clearly show that exposure to aluminium changes fusion pore properties by restraining its expansion. During kiss-and-run mode of exocytosis, vesicle cargo release is limited by the properties of the fusion pore through which cargo molecules diffuse from the vesicle lumen into the cell exterior (Barg *et al.*, 2002; Tsuboi and Rutter, 2003; Obermuller *et al.*, 2005). Actually, kinetics of fusion pore openings and widening are key constraints to achieve precise control of vesicle cargo discharge during kiss-and-run (Vardjan *et al.*, 2007a). Presently, a conclusive experimental demonstration of the mechanisms that regulate the dynamic behaviour of fusion pores remains to be achieved. On the other hand, multiple targets for an aluminium-induced alteration of neurotransmitter release have been proposed. The roles of G proteins, calcium channels and protein kinase C in the inhibitory effect of aluminium on glutamate release from transverse rat hippocampal slices have been emphasized by Provan and Yokel (1992). Interestingly, Scepek and co-workers (1998) showed that phorbol myristate acetate (PMA, activator of protein kinase C) and high intracellular Ca^{2+} concentrations could accelerate fusion pore expansion. In matter of fact, it seems that the fusion pore expansion rate is sensitive to intracellular free calcium in the range of micromolar concentrations (Fernández-Chacón and Alvarez de Toledo, 1995; Hartmann and Lindau, 1995). However, we observed that aluminium affects fusion pore properties of elementary regulated exocytotic events even under non stimulating conditions, rendering

difficult to explain how aluminium interferes with fusion pore widening by the light of the above mentioned studies.

In conclusion, the aluminium-induced changes in fusion of large dense-core vesicles with the plasma membrane of lactotrophs follow a consistent pattern of higher failure rates for productive exocytosis, mainly by preventing effective enlargement of fusion pores, hindering prolactin discharge from vesicular lumen to the extracellular space. The noticeable aluminium-induced switch to kiss-and-run fusion events characterised by fusion pores with diameter below 2.1 nm and no enhanced occurrence of fusion events in response to stimulation seems to reveal that large dense-core vesicles remain trapped in “kiss-and-run” mode of unproductive exocytosis upon exposure of rat pituitary lactotrophs-enriched cultures to sublethal concentration (30 μ M) of AlCl_3 during 24 h. Therefore, this effect might contributed to explain why significantly lower serum levels of prolactin in subjects with occupational exposure to aluminium have been found by Alessio and co-workers (1989).

4. References

- Alessio, L., Apostoli, P., Ferioli, A., Di Sipio, I., Mussi, I., Rigosa, C. 1989. Behaviour of biological indicators of internal dose and some neuro-endocrine tests in aluminium workers. *Med Lav* 80, 290–300.
- Allen, V. G., Fontenot, J. P., Rahnema, S. H. 1991. Influence of aluminum-citrate and citric acid on tissue mineral composition in wether sheep. *J Anim Sci.* 69, 792-800.
- Angleson JK, Betz WJ. Monitoring secretion in real time: capacitance, amperometry and fluorescence compared. *Trends Neurosci.* 20 (1997): 281-287
- Angleson, J., Cochilla, A., Kilic, G., Nussinovitch, I., Betz, W. 1999. Regulation of dense core release from neuroendocrine cells revealed by imaging single exocytotic events. *Nat Neurosci.* 2, 440-446.
- Barg S, Olofsson C, Schriever-Abeln J, Wendt A, Gebre-Medhin S, Renstrom E, Rorsman P (2002) Delay between fusion pore opening and peptide release from large-dense-core vesicles from neuroendocrine cells. *Neuron* 33: 287-299.
- Bauer RA, Overlease RL, Lieber JL, Angleson JK. Retention and stimulus-dependent recycling of dense core vesicle content in neuroendocrine cells. *J. Cell Sci.* 117 (2004) 2193-2202
- Ben-Jonathan, N., Hnasko, R. 2001. Dopamine as a prolactin (PRL) inhibitor. *Endocr Rev.* 22, 724-763.
- Ben-Tabou, S., Keller, E., Nussinovitch, I. 1994. Mechanosensitivity of voltage-gated calcium currents in rat anterior pituitary cells. *J Physiol.* 476, 29-39.
- Bole-Feysot, C., Goffin, V., Edery, M., Binart, N., Kelly, P. A. 1998. Prolactin (PRL) and its receptors: actions, signal transduction pathways and phenotypes observed in PRL receptor knockout mice. *Endocrine Reviews* 19, 225-268.

Chowdhury, H.H., Gabrjel, M., Grilc, S., Jorgacevski, J., Kreft, M., Pangrsic, T., Potokar, M., Stenovec, M., Vardjan, N., Zorec, R. 2006. Chapter 12 Exocytosis: The pulsing fusion pore. In: Liu A.L. (Eds.) *Advances in planar lipid bilayers and liposomes*, 5. Elsevier, USA.

Churchward, M.A., Rogasevskaia, T., Brandman, D.M., Khosravani, H., Nava, P., Atkinson, J.K., Coorssen, J.R. 2008. Specific lipids supply critical negative spontaneous curvature--an essential component of native Ca²⁺-triggered membrane fusion. *Biophys J.* 94, 3976-3986.

Cochilla AJ, Angleson JK, Betz WJ. Differential regulation of granule-to-granule and granule-to-plasma membrane fusion during secretion from rat pituitary lactotrophs. *J Cell Biol.* 150 (2000) 839-848; Pickett and Edwardson, 2006

Ebstein, R.P., Oppenheim, G., Ebstein, B.S., Amiri, Z., Stessman, J. 1986. The cyclic AMP second messenger system in man: the effects of heredity, hormones, drugs, aluminum, age and disease on signal amplification. *Prog Neuropsychopharmacol Biol Psychiatry.* 10, 323-353.

Erasmus, R.T., Savory, J., Wills, M.R., Herman, M.M. 1993. Aluminum neurotoxicity in experimental animals. *Ther Drug Monit.* 15, 588-592.

Fernández-Chacón, R., Alvarez de Toledo, G. 1995. Cytosolic calcium facilitates release of secretory products after exocytotic vesicle fusion. *FEBS Lett.* 363, 221-225.

Fernández-Martín, J.L., Canteros, A., Alles, A., Massari, P., Cannata-Andía, J. 2000. Aluminum exposure in chronic renal failure in iberoamerica at the end of the 1990s: overview and perspectives. *Am J Med Sci.* 320, 96-99.

Freeman, M. E., Kanyicska, B., Lerant, A., Nagy, G. 2000. Prolactin: Structure, Function and Regulation of Secretion. *Physiol Rev.* 80, 1523-1631.

Gonçalves, P.P., Silva, V.S. 2007. Does neurotransmission impairment accompany aluminium neurotoxicity? *J Inorg Biochem.* 101, 1291-1338.

Grishanin, R., Kowalchuk, J., Klenchin, V., Ann, K., Earles, C., Chapman, E., Gerona R., Martin, T. 2004. CAPS Acts at a Prefusion Step in Dense-Core Vesicle Exocytosis as a PIP2 Binding Protein. *Neuron*. 43, 551 - 562.

Haass NK, Kartenbeck MA, Leube RE. Pantophysin is a ubiquitously expressed synaptophysin homologue and defines constitutive transport vesicles. *J. Cell Biol.* 134 (1996) 731-746

Hartmann, J., Lindau, M. 1995. A novel Ca^{2+} -dependent step in exocytosis subsequent to vesicle fusion. *FEBS Lett.* 363, 217-220.

Haug, A., Shi, B., Vitorello, V. 1994. Aluminum interaction with phosphoinositide-associated signal transduction. *Arch Toxicol.* 68, 1-7. Review.

Jankowska, A., Madziar, B., Tomaszewicz, M., Szutowicz, A. 200. Acute and chronic effects of aluminum on acetyl-CoA and acetylcholine metabolism in differentiated and nondifferentiated SN56 cholinergic cells. *J Neurosci Res.* 62, 615-622.

Julka, D., Gill, K.D. 1996. Altered calcium homeostasis: a possible mechanism of aluminium-induced neurotoxicity. *Biochim Biophys Acta.* 1315, 47-54.

Kanaho, Y., Moss, J., Vaughan, M. 1985. Mechanism of inhibition of transducin GTPase activity by fluoride and aluminum. *J Biol Chem.* 260, 11493-11497.

Klyachko, V.A., Jackson, M.B. 2002. Capacitance steps and fusion pores of small and large-dense-core vesicles in nerve terminals. *Nature.* 418, 89-92.

Kopeloff, N., Whittier, J.R., Pacella, B.L., Kopeloff, L.M. 1950. The epileptogenic effect of subcortical alumina cream in the rhesus monkey. *Electroencephalogr. Clin. Neurophysiol.* 2, 163–168.

Kozlovsky, Y., Chernomordik, L.V., Kozlov, M.M. 2002. Lipid intermediates in membrane fusion: formation, structure, and decay of hemifusion diaphragm. *Biophys J.* 83, 2634-2651.

Kreft, M., Zorec, R. 1997. Cell-attached measurements of attofarad capacitance steps in rat melanotrophs. *Pflugers Arch.* 434, 212-214.

Lledo, P.M., Vernier, P., Vincent, J.D., Mason, W.T., Zorec, R. 1993. Inhibition of Rab3B expression attenuates Ca^{2+} -dependent exocytosis in rat anterior pituitary cells. *Nature.* 364, 540-544.

Lollike, K., Lindau, M. 1999. Membrane capacitance techniques to monitor granule exocytosis in neutrophils. *J Immunol Methods.* 232, 111–120.

Loyet, K.M., Kowalchyk, J.A., Chaudhary, A., Chen, J., Prestwich, G.D., Martin, T.F. 1998. Specific binding of phosphatidylinositol 4,5-bisphosphate to calcium-dependent activator protein for secretion (CAPS), a potential phosphoinositide effector protein for regulated exocytosis. *J Biol Chem.* 273, 8337-8343.

MacLeod, R.M., Lehmeier, J.E. 1974. Studies on the mechanism of the dopamine-mediated inhibition of prolactin secretion. *Endocrinology.* 94, 1077-85.

Neher, E., Marty, A. 1982. Discrete changes of cell membrane capacitance observed under conditions of enhanced secretion in bovine adrenal chromaffin cells. *Proc Natl Acad Sci USA* 79, 6712-6716.

Neher, E. 1998. Vesicle pools and Ca^{2+} microdomains: new tools for understanding their roles in neurotransmitter release. *Neuron.* 20, 389-399.

Nostrandt, A.C., Shafer T.J., Mundy W.R., PADILLA, S. 1996. Inhibition of Rat Brain Phosphatidylinositol-Specific Phospholipase C by Aluminum: Regional Differences, Interactions with Aluminum Salts, and Mechanisms. *TOXICOLOGY AND APPLIED PHARMACOLOGY* 136, 118 -125.

Obermüller S, Lindqvist A, Karanauskaite J, Galvanovskis J, Rorsman P, Barg S (2005) Selective nucleotide-release from dense-core granules in insulin-secreting cells. *J Cell Sci* 118:4271-4282.

Ohba, S., Hiramatsu, M., Edamatsu, R., Mori, I., Mori, A. 1994. Metal ions affect neuronal membrane fluidity of rat cerebral cortex. *Neurochem Res.* 19, 237-241.

Seino, S., Shibasaki, T. 2005. PKA-Dependent and PKA-Independent Pathways for cAMP-Regulated Exocytosis. *Physiol Ver.* 85, 1303-1342.

Pandya, J.D., Dave, K.R., Katyare, S.S. 2004. Effect of long-term aluminum feeding on lipid/phospholipid profiles of rat brain myelin. *Lipids Health Dis.* 22, 3-13.

Pow DV, Morris JF. Membrane routing during exocytosis and endocytosis in neuroendocrine neurones and endocrine cells: use of colloidal gold particles and immunocytochemical discrimination of membrane compartments. *Cell Tissue Res.* 264 (1991) 299-316

Provan, S.D., Yokel, R.A. 1992. Aluminum inhibits glutamate release from transverse rat hippocampal slices: role of G proteins, Ca channels and protein kinase C. *Neurotoxicology.* 13, 413-420.

Sarin, S., Gupta, V., Gill, K.D. 1997. Alterations in lipid composition and neuronal injury in primates following chronic aluminium exposure. *Biol Trace Elem Res.* 59, 133-143.

Scepek, S., Coorssen, J.R., Lindau, M. 1998. Fusion pore expansion in horse eosinophils is modulated by Ca²⁺ and protein kinase C via distinct mechanisms. *EMBO J.* 17, 4340-4345.

Senda T, Ochiai H, Nakai Y, Fujita H. Immunocytochemical localization of synaptophysin (protein p38) and synapsin I in nerve terminals of rat neurohypophysis. *Arch Histol Cytol.* 54 (1991) 233-240

Shafer, T.J., Mundy, W.R. 1995. Effects of aluminum on neuronal signal transduction: mechanisms underlying disruption of phosphoinositide hydrolysis. *Gen Pharmacol.* 26, 889-895. Review.

Shi, B., Chou, K., Haug, A. 1993. Aluminium impacts elements of the phosphoinositide signalling pathway in neuroblastoma cells. *Mol Cell Biochem.* 121,109-118.

Siegel, N., Haug, A. 1983. Aluminum interaction with calmodulin. Evidence for altered structure and function from optical and enzymatic studies. *Biochim Biophys Acta.* 744, 36-45.

Sikdar, S.K., Kreft, M., Zorec, R. 1998. Modulation of unitary exocytotic event amplitude by cAMP in rat melanotrophs. *J Physiol.* 511, 851-859.

Silva, V.S., Cordeiro, J.M., Matos, M.J., Oliveira C.R., Gonçalves P.P. 2002. Aluminium accumulation and membrane fluidity alteration in synaptosomes isolated from brain cortex following aluminium ingestion: effect of cholesterol. *Neuroscience Research* 44, 181-193.

Silva, V.S., Nunes, M.A., Cordeiro, J.M., Calejo, A.I., Santos, S., Neves, P., Sykes, A., Morgado, F., Dunant, Y., Gonçalves, P.P. 2007. Comparative effects of aluminum and ouabain on synaptosomal choline uptake, acetylcholine release and (Na⁺/K⁺)ATPase. *Toxicology.* 236, 158-77.

Smets, G., Velkeniers, B., Finne, E., Baldys, A., Gepts, W., Vanhaelst, L. 1987. Postnatal development of growth hormone and prolactin cells in male and female rat pituitary. An immunocytochemical light and electron microscopic study. *J Histochem Cytochem.* 35, 335– 341.

Stenovec, M., Kreft, M., Poberaj, I., Betz, W., Zorec, R. 2004. Slow spontaneous secretion from single large dense-core-vesicles monitored in neuroendocrine cells. *FASEB J* 18, 1270-1272.

Stojilkovic, S.S. 2005. Ca²⁺-regulated exocytosis and SNARE function. *Trends Endocrinol Metab.* 16, 81-3.

Spruce A, Breckenridge L, Lee A, Almers W (1990) Properties of the fusion pore that forms during exocytosis of a mast cell secretory vesicle. *Neuron* 4:643-654.

Sweeney, V.P., Perry, T.L., Price, J.D., Reeve, C.E., Godolphin, W.J., Kish, S.J. 1985. Brain gamma-aminobutyric acid deficiency in dialysis encephalopathy. *Neurology* 35, 180–184.

Szutowicz, A., Bielarczyk, H., Kisielewski, Y., Jankowska, A., Madziar, B., Tomaszewicz, M. 1998. Effects of aluminum and calcium on acetyl-CoA metabolism in rat brain mitochondria. *J Neurochem.* 71, 2447-2453.

Tsuboi T & Rutter G (2003) Multiple forms of "kiss-and-run" exocytosis revealed by evanescent wave microscopy. *Curr Biol* 13:563-567.

Tsunoda, M., Sharma, R.P. 1999. Altered dopamine turnover in murine hypothalamus after low-dose continuous oral administration of aluminum. *J Trace Elem Med Biol.*13, 224-231.

Turgeon, J.L., Shyamala, G., Waring, D.W. 2001. PR localization and anterior pituitary cell populations in vitro in ovariectomized wild-type and PR-knockout mice. *Endocrinology.* 142, 4479-4485.

Vardjan, N., Stenovec, M., Jorgacevski, J., Kreft, M., Zorec, R. 2007a. Subnanometer fusion pore in spontaneous exocytosis of peptidergic vesicles. *J Neurosci.* 27, 4737-4746.

Vardjan, N., Stenovec, M., Jorgacevski, J., Kreft, M., Zorec, R. 2007b. Elementary properties of spontaneous fusion of peptidergic vesicles: fusion pore gating. *The Journal of Physiology,*

Verstraeten, S.V., Oteiza, P.I. 2002. Al(3+)-mediated changes in membrane physical properties participate in the inhibition of polyphosphoinositide hydrolysis. *Arch Biochem Biophys.* 408, 263-271.

Walton, J.R. 2004. A bright field/fluorescent stain for aluminum: its specificity, validation, and staining characteristics. *Biotechnic and Histochemistry.* 79, 169-176.

Zatta, P., Zambenedetti, P., Reusche, E., Stellmacher, F., Cester, A., Albanese, P., Meneghel, G., Nordio, M. 2004. A fatal case of aluminium encephalopathy in a patient with severe chronic renal failure not on dialysis. *Nephrol Dial Transplant.* 19, 2929-2931.

Zatta, P., Nicosia, V., Zambenedetti, P. 1998. Evaluation of MAO activities on murine neuroblastoma cells upon acute or chronic treatment with aluminium (III) or tacrine. *Neurochem Int.* 32, 273-279.

Zimmerberg, J., Chernomordik, L.V. 1999. Membrane fusion. *Adv Drug Deliv Rev.* 38, 197-205.

Zubenko, G.S., 1990. Significance of increased platelet membrane fluidity in mental disorders of late-life. *Ups. J. Med. Sci.* 48, 225-244.

III. Conclusions

A long way has passed since the first report about aluminium neurotoxicity. Nowadays the effect of aluminium in multiple organs it is unquestionable. Neurobehavioral alteration and neurodegeneration following aluminium exposure are well documented. However, a great amount of what has been reported about the molecular mechanism of aluminium neurotoxicity still controversial. In this work carried out with rat anterior pituitary lactotrophs enriched cultures we demonstrated that:

1. Submillimolar levels of aluminium induce cell death. This effect is concentration and time dependent as revealed by dual-labeling flow cytometric analysis using calcein AM and ethidium homodimer.
2. Accumulation of Al^{3+} in cells occurs prior to massive cell lost as evaluated by graphite furnace atomic absorption spectrometry.
3. Aluminium, in the micromolar range of concentrations, prevents exocytotic response to stimulation with high K^+ and alters the properties of elementary exocytotic events by enhancing the fraction of events with lowest measurable fusion pore when studied by membrane capacitance recording performed with a dual-phase lock-in patch-clamp amplifier in the cell-attached patch-clamp configuration.

The results suggest that exposure to aluminium can reduce the supply of mammalian neuroendocrine hormone prolactin from pituitary lactotrophs.